Exploitation of host chemokine signalling by pathogenic mycobacteria

Torraca, V.

Chapter 5

CRISPR/Cas9 mutagenesis of zebrafish Cxcr3.3 suggests opposing functions of atypical and canonical Cxcr3 paralogues on mycobacterial infection control

Vincenzo Torraca, Frida Sommer, Sarah Kamel, Natasja A. Otto and Annemarie H. Meijer

Institute of Biology, Leiden University, The Netherlands

Chapter 5

CRISPR/Cas9 mutagenesis of zebrafish Cxcr3.3 suggests opposing functions of atypical and canonical Cxcr3 paralogues on mycobacterial infection control

Vincenzo Torraca, Frida Sommer, Sarah Kamel, Natasja A. Otto and Annemarie H. Meijer

Institute of Biology, Leiden University, The Netherlands

Zebrafish immune cells express three homologues of the human chemokine receptor CXCR3. We have recently shown that one of these homologues, Cxcr3.2, plays an important role in macrophage migration and dissemination of mycobacterial infection, suggesting that inhibition of CXCR3 signalling could be used as a host-directed therapeutic strategy for treatment of tuberculosis. However, the functions of the other CXCR3 isoforms in zebrafish remain to be elucidated. Here, we successfully applied CRISPR/Cas9 genome editing tools to obtain non-sense mutants of the *cxcr3.3* gene. Additionally, we introduced several optimisations to the CRISPR/Cas9 editing system that facilitated an efficient application of the method in terms of time, costs and yield. As a result, *cxcr3.3* was efficiently mutated in 70% of injected embryos, leading to a similar yield of adult germ-line mosaic carriers. Initial characterisation of *cxcr3.3* mutants revealed that homozygote mutation is viable, does not provoke evident discomfort to the carriers and is maintained according to Mendelian proportions. When tested in the zebrafish tuberculosis model, *cxcr3.3* mutants displayed an increased burden of mycobacterial infection. Unexpectedly, this phenotype is opposite to that of *cxcr3.2* mutants that more efficiently counteract initial mycobacterial replication and mycobacterial dissemination in the granulomatous stage. Sequence analysis of CXCR3 from fish and other vertebrates revealed that Cxcr3.3 in zebrafish may function as an atypical chemokine receptor (ACKR), since it displays replacement of key amino acid residues essential to mediate the activation of heterotrimeric G-proteins. Notably, the presence of atypical Cxcr3 receptors appears conserved among fish species, although it was possibly lost at the radiation of tetrapods, since only classical CXCR3 receptors are present in amphibians, reptiles and mammals. This suggests that Cxcr3.3 may exert a regulatory function on Cxcr3.2 signalling by scavenging/competition for ligands. Further mechanistic studies should be performed to validate this hypothesis and to analyse the cross-talk between Cxcr3.2 and Cxcr3.3 receptors.

GRAPHICAL ABSTRACT

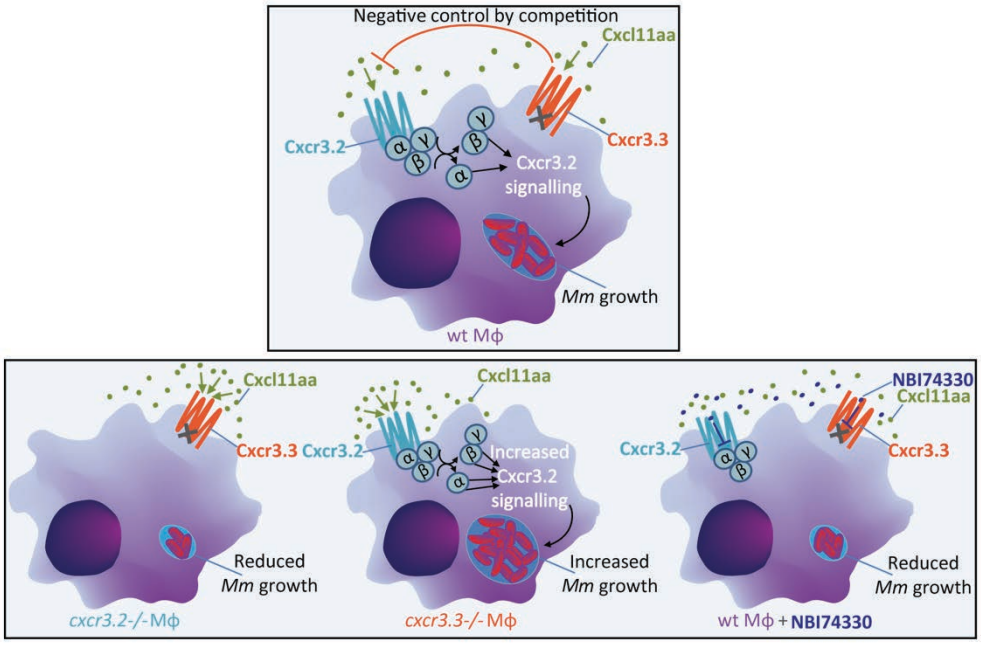

Zebrafish macrophages express both Cxcr3.2 and Cxcr3.3 receptors. Cxcr3.2 is able to evoke macrophage chemotaxis via its Cxcl11 cognate ligands and contains an intact DRY (Asp-Arg-Tyr) motif, which would permit its coupling with downstream G-protein signalling. Upon ligand binding to the receptor, heterotrimeric G-proteins would dissociate into Gα and Gβγ subunits and modulate the activity of their targets. We previously showed that Cxcr3.2-mediated signalling leads to increased susceptibility to mycobacterial infection and abolishment of this signalling benefits the host. We show here that unlike Cxcr3.2, Cxcr3.3 does not contain a DRY motif, suggesting that this receptor is unable to direct G-protein coupled receptor signalling, similarly to other atypical chemokine receptors. Additionally, *cxcr3.3* mutations increase susceptibility to infection. In our proposed model, wt Cxcr3.3 expression may exert a beneficial function by scavenging Cxcr3.2 ligands, therefore limiting activation of Cxcr3.2 pro-infection downstream signalling. That Cxcr3.3 requires simultaneous Cxcr3.2 expression to exert its function is also suggested by treatment with NBI74330, a CXCR3 antagonist that is thought to block both Cxcr3.2 and Cxcr3.3. In this situation, the susceptibility to infection is attenuated, phenocopying *cxcr3.2* mutation and not *cxcr3.3* mutation.

INTRODUCTION

Chemokines constitute a family of potent chemotactic molecules which play complex pleiotropic functions in the control of the immune response and of host-pathogen interactions[1]. The zebrafish (*Danio rerio*) is an attractive vertebrate model to study this complexity *in vivo,* as it provides both a genetically tractable system, to generate new genetically-encoded tools, and an optically-accessible platform to follow the dynamics of immune cells and processes intravitally[2]. The genetic tractability of zebrafish enabled generation of a multitude of transgenic and mutant lines of interest for the immune system and in particular to study chemokine receptors, a class of 7-loop transmembrane (7TM) and G-protein coupled receptors (GPCR) that signal via their cognate chemokine ligands. For example, wildtype (wt) and mutated versions of Cxcr4b have been fused with fluorescent proteins to study receptor expression/internalisation dynamics and its function in controlling cell migration and phagocyte mobilisation[3,4]. Random mutagenesis screening programmes[5] have provided widely used null chemokine ligand and receptor mutants, such as *cxcl12a*[6], *cxcr4b*[7], *cxcr7b*[8] (also known as atypical chemokine receptor 3b, *ackr3b*), and *cxcr3.2*[9]. These mutants, used in combination with transgenic reporters that allow differential labelling of immune cell types, have been critical for *in vivo* analysis of immune responses and cell motility.

Recent advances in genome editing strategies provided the possibility to specifically target genes of interest, including chemokine ligands and receptors[10,11]. As a consequence, these technologies are contributing to greatly expand the array of genetic tools available to the zebrafish field. State-of-the-art genome editing techniques include zinc finger nucleases (ZFN), transcription activator-like effector nucleases (TALEN), and clustered regularly interspaced short palindromic repeats-associated protein 9 (CRISPR/Cas9) technology[12,13,14]. All these techniques have been efficiently applied to zebrafish genome editing, for both insertion of transgenic constructs and generation of transmissible mutations[15,16,17,18]. However, CRISPR/Cas9 technology has several advantages when compared to ZFN and TALEN techniques and is, therefore, becoming the predominantly used method for genome manipulation[13]. In both ZFNs and TALENs, recognition of the DNA target site and the endonuclease activity are driven by specific protein domains. However, in CRISPR/Cas9 technology, recognition of the target depends on a short guide RNA (shgRNA) which pairs to the target site by nucleotide matches, while the actual endonuclease activity is catalysed by a universal Cas9 protein, driven to the target site by matching to a constant region of the shgRNA (**Figure 1**).

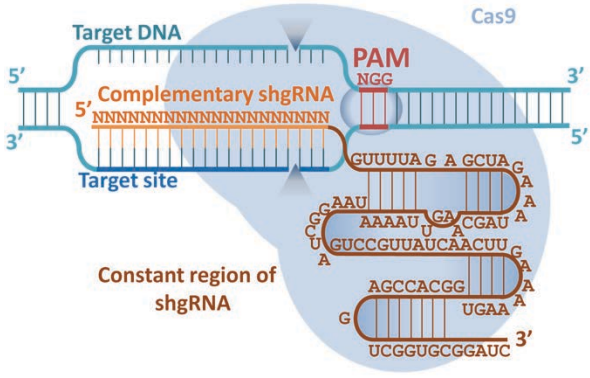

Figure 1. Schematic representation of the CRISPR/Cas9 system. The system uses a nuclease, CRISPR-associated 9 (Cas9), that complexes with short guide RNAs (shgRNAs) to cleave DNA in a sequence-specific manner upstream of the protospacer adjacent motif (PAM) in any genomic location. The endogenous CRISPR-Cas9 system is comprised of 2 separate guide RNAs known as the crRNA and tracrRNA. In the bioengineered version of the system, these two separate RNAs have been combined into a single guide RNA. Adapted from reference[14].

Because of this difference, the construction of ZFN and TALEN nucleases requires complex and laborious multistep cloning strategies or acquisition of costly synthetic constructs to build up the DNA templates encoding the target-specific ZFN/TALEN recognition protein domains. A major advantage of CRISPR/Cas9 technology is that it requires only simple molecular biology tools (primers/short oligo templates or simple cloning procedures) to engineer the shgRNA template responsible for the base-pairing-dependent target recognition.

In the CRISPR/Cas9 protocol used in this study, the shgRNA consists of 101 bases with a 20-nucleotide-long sequence complementary to the DNA target site (at its 5' extremity) (**Figure 1**)[12,13]. This sequence is fundamental for the target recognition via base-pairing. The remaining shgRNA sequence contains the RNA hairpins required to form a complex with the Cas9 endonuclease. Cas9 does not participate in the recognition of the 20-base target site; however, it requires that the target site is followed by a Protospacer Adjacent Motif (PAM) sequence (most commonly 5'-NGG-3')[12,13]. The PAM sequence provides an anchoring site, which is fundamental for efficient cleavage. Following recognition of the target site, a double strand break will be generated within the genomic target site, most likely three nucleotides upstream of the PAM sequence. The 8-12 bases immediately upstream of the PAM motif represent the "seeding sequence" and any mismatches in this region will abolish shgRNA/Cas9 activity. Mismatches beyond this nucleotide sequence are generally tolerable[12,13]. This has a direct impact on the specificity and on off-target effects that the CRISPR/Cas9 technique might have, compared with other gene editing techniques which generally require recognition of longer consensus sequences. However, a new variant of high fidelity Cas9, carrying sequence optimisations designed to reduce non-specific DNA contacts, is already available and appears to not provoke any detectable off-target effects[19]. Due to its simple approach, high efficiency and low costs, the CRISPR/Cas9 technique is becoming the elective technique for genome editing.

Like other teleosts, zebrafish have experienced three rounds of whole genome duplication (WGD) resulting in an increase of the copy number of several genes[20]. Moreover, some further zebrafish-specific chemokine gene cluster expansions have been observed. Comparative analysis of the zebrafish and human genomes revealed that whilst there are at least 36 putative chemokine receptors and 75 putative chemokine ligands in zebrafish, only 25 chemokine receptors and 45 chemokine ligands have been mapped to the human genome[20]. The CXC-motif subfamily of chemokine receptors and ligands (CXCRs/CXCLs) is involved in multiple processes, spanning from the trafficking of leukocytes to the regulation of angiogenesis. These CXCR/CXCL subfamilies are less divergent between lower vertebrates and mammals, compared with other chemokine ligand and receptor families. For example, at least 11 canonical CXCRs and 20 CXCLs have been identified in zebrafish, versus 7 canonical CXCRs and 17 CXCLs described in humans[20].

Several cases of functional and ligand/receptor partnership conservation have been described for the zebrafish and mammalian CXCR/CXCL counterparts. CXCR2/CXCL8 signalling leads to the chemoattraction of human neutrophils and their recruitment to inflamed sites[21,22]. Notably, an orthologous Cxcr2/Cxcl8a signalling axis exists in zebrafish[23], while this powerful neutrophil chemoattractant signal is not represented in rodents[24,25]. CXCR4/CXCL12 interaction is involved in haematopoietic stem cell (HSC) and leukocyte mobilisation/homoeostasis[26,27], in cancer and HIV pathogenesis[28,29]. Similarly, the Cxcr4b/Cxcl12a zebrafish axis recapitulates several conserved roles in innate

immunity, such as the retention of neutrophils and macrophages in haematopoietic tissues[4], recruitment of HSCs to the definitive sites of haematopoiesis[30] and in metastasis of cancer xenografts[31]. The CXCR4/CXCL12 axis is duplicated in zebrafish and a Cxcr4a/Cxcl12b axis also exists[32]. However, the two seemingly redundant systems experience sub-functionalisation and each control specific functions played by their mammalian CXCR4/CXCL12 counterpart. Notably, while disruption of this axis is embryonic lethal in mammals[33,34,35] the partial redundancy of the CXCR4/CXCL12 system permits the existence of viable knockouts, displaying attenuated and more specific phenotypes, which proved extremely useful to study particular aspects regulated by this axis *in vivo*.

CXCR3 is expressed by different types of leukocytes, including T lymphocytes, natural killer cells, macrophages and dendritic cells and plays an important part in trafficking and function of these cell types in inflammatory and autoimmune diseases[36,37,38,39]. The ligand of this receptor in mammals is represented by a triplet of inflammatory chemokines, namely CXCL9-10-11. In zebrafish, three copies of this gene are present, *cxcr3.1, cxcr3.2, cxcr3.3* (**Figure 2A**)[9]. Of these three isoforms, only *cxcr3.2* has been recently characterised, as being involved in controlling the microbicidal capability of macrophages[40], the migration of macrophages to infection foci, and macrophage-mediated dissemination of mycobacterial infection[9]. It is still unknown whether the other two isoforms have complementary/redundant functions. Likewise, the cluster of CXCL9-10-11 chemokines (which represent the class of interacting partners of CXCR3-like receptors) is also expanded in zebrafish and includes 7 ligands, namely Cxcl11aa-ac-ad-ae-af-ag-ah[9,20]. While the sole human CXCR3 responds to CXCL9-10-11, it seems that not all the zebrafish Cxcl11 ligands are able to elicit a Cxcr3.2-dependent response[9]. Cxcl11aa and Cxcl11af were shown to mobilise macrophages via Cxcr3.2, while Cxcl11ae was able to comparably recruit macrophages also in the *cxcr3.2* null mutants. This suggests that Cxcr3.1, Cxcr3.2 and Cxcr3.3 and their ligand partners are not completely redundant and interchangeable, similar to the Cxcr4a/b/Cxcl12a/b system[32]. RNA-sequencing and qRT-PCR data of Fluorescence-Activated Cell Sorting (FACS) of macrophages, neutrophils and immature T cells revealed that *cxcr3.1* was only detectable in immature T cells, while *cxcr3.2* and *cxcr3.3* were significantly expressed by both macrophages and neutrophils[9,41], suggesting cell-type functional specialisation.

Our previous analysis of a zebrafish *cxcr3.2* mutant in the zebrafish embryo model for tuberculosis suggested that inhibition of CXCR3 signalling could be used as a host-directed therapeutic strategy for treatment of the mycobacterial infection causing this disease[9]. As mentioned above, *cxcr3.2* and *cxcr3.3* display a similar macrophage and neutrophil-specific expression profile in the embryo model. Since a *cxcr3.3* mutant was not available and the function of this gene in recruitment, development and mobilisation of immune cells is unknown, we aimed here to apply CRISPR/Cas9 technology to disrupt *cxcr3.3*. We additionally present our own adaptations to the CRISPR/Cas9 method which allowed synthesis of shgRNAs from a PCR-based template and *in vivo* selection of target sites with high mutagenesis efficiency. Finally, we present a preliminary characterisation of the *cxcr3.3* mutants we obtained in the zebrafish tuberculosis model. Notably, *cxcr3.3* mutation revealed the opposite effect to that seen in the context of *cxcr3.2* mutation. Interestingly, *cxcr3.3* does not contain the DRY (Asp-Arg-Tyr) motif, which is fundamental to transduce GPCR signalling, which suggests that this receptor may act as an atypical chemokine receptor. These findings emphasise the need for an in-depth

characterisation of cross talk between Cxcr3.2 and Cxcr3.3 in controlling host-pathogen interactions.

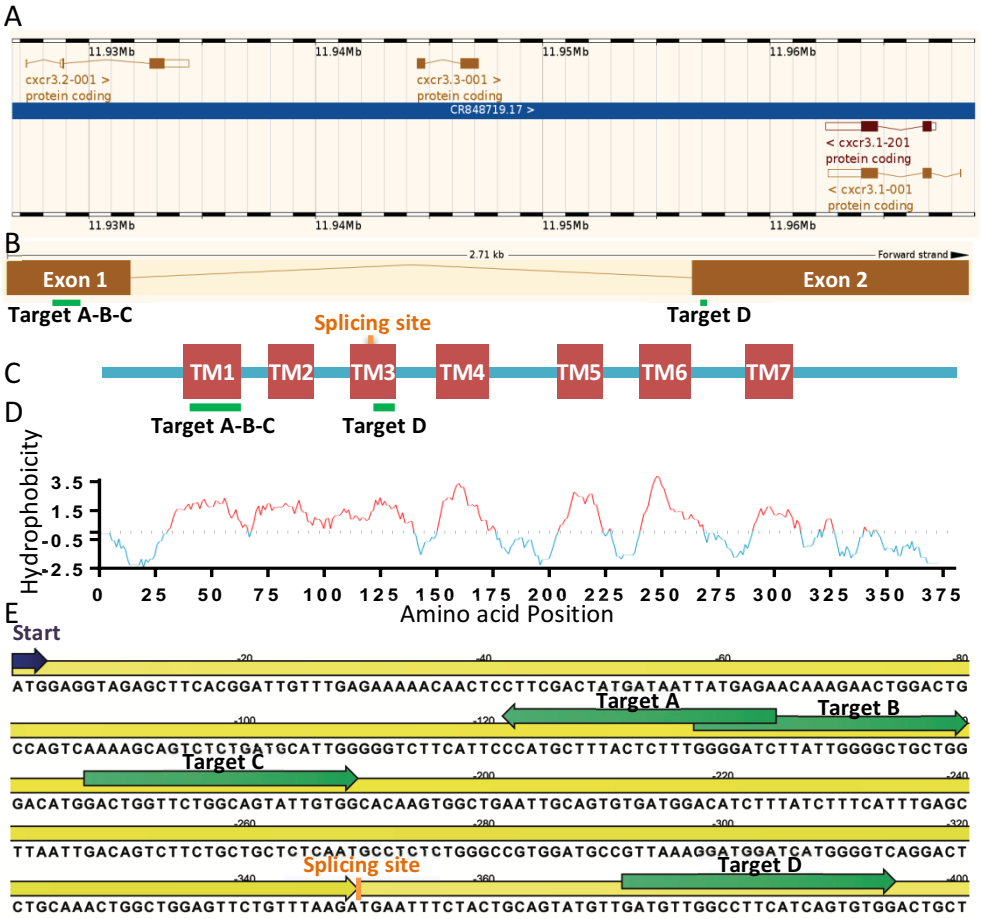

Figure 2. Design of CRISPR targets for *cxcr3.3*. A. Genomic locus of *cxcr3* zebrafish genes. The zebrafish genomic locus Chr16:11926632-11969001 (contig CR848719.17, zebrafish genome version GRCz10) contains three mammalian CXCR3 orthologues *cxcr3.1*, *cxcr3.2*, and *cxcr3.3*. **B-C.** Genomic and encoded protein architecture of the *cxcr3.3* locus. The *cxcr3.3* gene spans 2.71 kb and consists of two exons. Exon 1 encodes the N-terminal extracellular domain, the transmembrane domains TM1, TM2, and part of TM3; exon 2 codes for the remaining part of TM3, for TM4, TM5, TM6, TM7 and for the C-terminal intracellular domain. Lines in green depict the position of the CRISPR Targets A, B, C and D. **D.** Prediction of the TM domains was computed with an online transmembrane prediction tool (http://www.ch.embnet.org/cgi-bin/TMPRED_form_parser), based on the hydrophobicity plot and is consistent with the conventional structure of a seven loop transmembrane receptor. **E.** Nucleotide sequence of *cxcr3.3* in the region containing the targeting sites. Target sites are marked in green. The ATG codon in represented in violet and the splicing site is represented by a yellow bar.

RESULTS

CRISPR target design

There are several bioinformatic tools available to design CRISPR targets. Finding a putative target site is simple since virtually any genomic 5'-$(N)_{21}$GG-3' sequence is a possible site for CRISPR targeting (**Figure 1**). However, since the synthesis or shgRNA implies transcription from a T7 promoter and since T7 RNA-polymerase most preferably initiates transcription from a G, this forces the design of efficiently transcribed targets to respect the 5'-G$(N)_{20}$GG-3' sequence constraint. Notably, other transcription promoters may be used to drive expression of the shgRNA (e.g. U6, SP6), which would not require the presence of a G at the +1 position. Likewise, recently novel versions of Cas9 (derived from other bacteria and requiring alternative PAM sequences) are also available. Therefore, if necessary, alternative designs are possible. Apart from the transcription-related and Cas9-related constraints, many other filtering criteria apply when selecting a target site. These include the intronic-exonic architecture, the probability of epigenetic modification/accessibility of the target at the genomic site, the GC content, the specificity of the target site/probability of off-target effects, the existence of self-complementarities and secondary structures in the shgRNA. Therefore, different online tools provide a classification of the targets according to scoring criteria that take into account several variables.

To target *cxcr3.3*, we selected 4 candidate target sequences, respecting the 3'-G$(N)_{20}$GG-5' signature and falling into a relatively proximal region of the coding sequence of *cxcr3.3* (within 396 dNTPs/132 aa from the translation start) (**Figure 2B-E** and **Table 1**). The first 2 targets (Target A and B) were obtained using a CRISPR/Cas9-dedicated engine from ZiFiT Targeter Version 4.2 (http://zifit.partners.org/ZiFiT/CSquare9Nuclease.aspx). The other two targets (Targets C and D) were obtained as 2 top scoring hits by the CHOPCHOP web-tool (https://chopchop.rc.fas.harvard.edu/index.php)[42]. ZiFit does not provide any support in the selection of the targets, based on their properties. Therefore, the list of putative targets was screened manually, based on proximity of the target to the 5' end of *cxcr3.3* and on the presence of putative off-targets. Differently, the CHOPCHOP web-tool uses a specific algorithm that scores and ranks potential target sites[42]. A Bowtie-based alignment system (an ultrafast and efficient algorithm to align short sequences to full genomes[43]) allows the identification of the most specific target sites. Target sites are therefore ranked based on number of off-targets, number of mismatches (when searching for putative off-targets), proximity of the target site to the ATG of translation start (the more proximal, the better), GC content (best if 50-60%), and the presence of a G at position 20 (which appears to improve the cutting rate[44]). For comparison, we also used a published target for *eGFP*[15] (**Table 1**), aiming to assay by fluorescence the efficiency of the CRISPR knockout by mutation of an eGFP transgene from a zebrafish transgenic line (*Tg(fli1a:eGFP)*[45], see results sections for explanation and further details).

Preparation of shgRNA

Most of recent reports used a cloning-based strategy to obtain a DNA template for *in vitro* transcription of shgRNA[16,46,47.48,49,50,51]. However, few reports have indicated that short transcripts can be also transcribed with cloning-free systems based on synthetic DNA oligonucleotide templates[15,17,52,53]. This second option appears more desirable, since it would facilitate and accelerate the synthesis process, and is suited to set up a standardised

method that can be immediately adapted for targeting new genes of interest or to carry multiple targets at once. The downside of the oligonucleotide-based synthetic strategies versus the plasmid-based ones may be the limited yield of templates, the large costs of synthesis and the poor transcription efficiency to obtain the final RNA product. In order to identify the most efficient system to obtain shgRNA, we compared three different sources of DNA template (**Figure 3**): full-length (122-bases) synthetic single-stranded DNA (ssDNA) template (Method 1); dsDNA derived from a PCR-based complementation and amplification of full-length (122-bases) synthetic ssDNA oligonucleotide (Method 2); dsDNA template derived from PCR-based complementation and amplification of two 81-base-long semi-complementary oligonucleotides (Method 3). Although the T7 RNA polymerase does not require a dsDNA template, it requires the T7 promoter site to be double-stranded[,54]. Therefore, for Method 1, RNA was transcribed upon annealing of an equimolar concentration of T7 primer, in order to complement the T7 promoter site (See Materials and Methods for more details). Comparing the yields of shgRNA product obtained with the 3 methods, we found that the Method 1 was extremely inefficient, yielding < 0.2 µg of total RNA. Method 2 and 3 had comparable efficiencies, yielding over 40 µg of total RNA product (**Table 2**). Between Method 2 and 3, we found Method 3 technically more convenient. Since the target site-specific sequence is localised at the 5' extremity of the DNA template, it could be confined entirely into the forward 81-mer oligonucleotide. This means that the reverse 81-mer oligonucleotide matches exclusively to the constant shgRNA region (common to any shgRNAs). Synthesis of >100 bp synthetic oligos (Method 1 and 2) is costly, takes longer delivery time, requires polyacrylamide gel electrophoresis (PAGE)-based purification, and is more prone to introduction of sequence errors. This is particularly true for a shgRNA template, that includes long stretches of repetitive nucleotides. By using Method 3, we could avoid ordering of a new 122-mer for each CRISPR and could minimise the order to 1 single 81-mer oligo for each new CRISPR.

	Target site, 5' to 3'	Orientation	Position
***cxcr3.3* Target A**	GATCCCCAAAGAGTAAAGCATGG	Reverse strand	122-144
***cxcr3.3* Target B**	GGGGATCTTATTGGGGCTGCTGG	Forward strand	138-160
***cxcr3.3* Target C**	GACTGGTTCTGGCAGTATTGTGG	Forward strand	167-189
***cxcr3.3* Target D**	GATGTTGGCCTTCATCAGTGTGG	Forward strand	372-394
***eGFP* Target**	GGGCACGGGCAGCTTGCCGGTGG	Reverse strand	149-171

Table 1. Target sites used in this study. Underlined NGG sequences represent the PAM consensus. Positions are relative to the translational Start and refer to the cDNA sequence.

	eGFP Target	*cxcr3.3* Target A	*cxcr3.3* Target B	*cxcr3.3* Target C	*cxcr3.3* Target D
Method 1	<10	<10	<10	-	-
Method 2	1968.3	3023.0	1850.5	-	-
Method 3	-	-	-	1627.4	2514.5

Table 2. Yields (ng/µl) of the different methods used in this study. Concentration refers to 20 µl transcription reactions performed with 100 ng of ssDNA (Method 1) or 200 ng of dsDNA template (Methods 2-3). Upon column cleanup, RNA was eluted in 20 µl (2x10 µl) of RNAse-free water. 1 µl was used for nanodrop measurement.

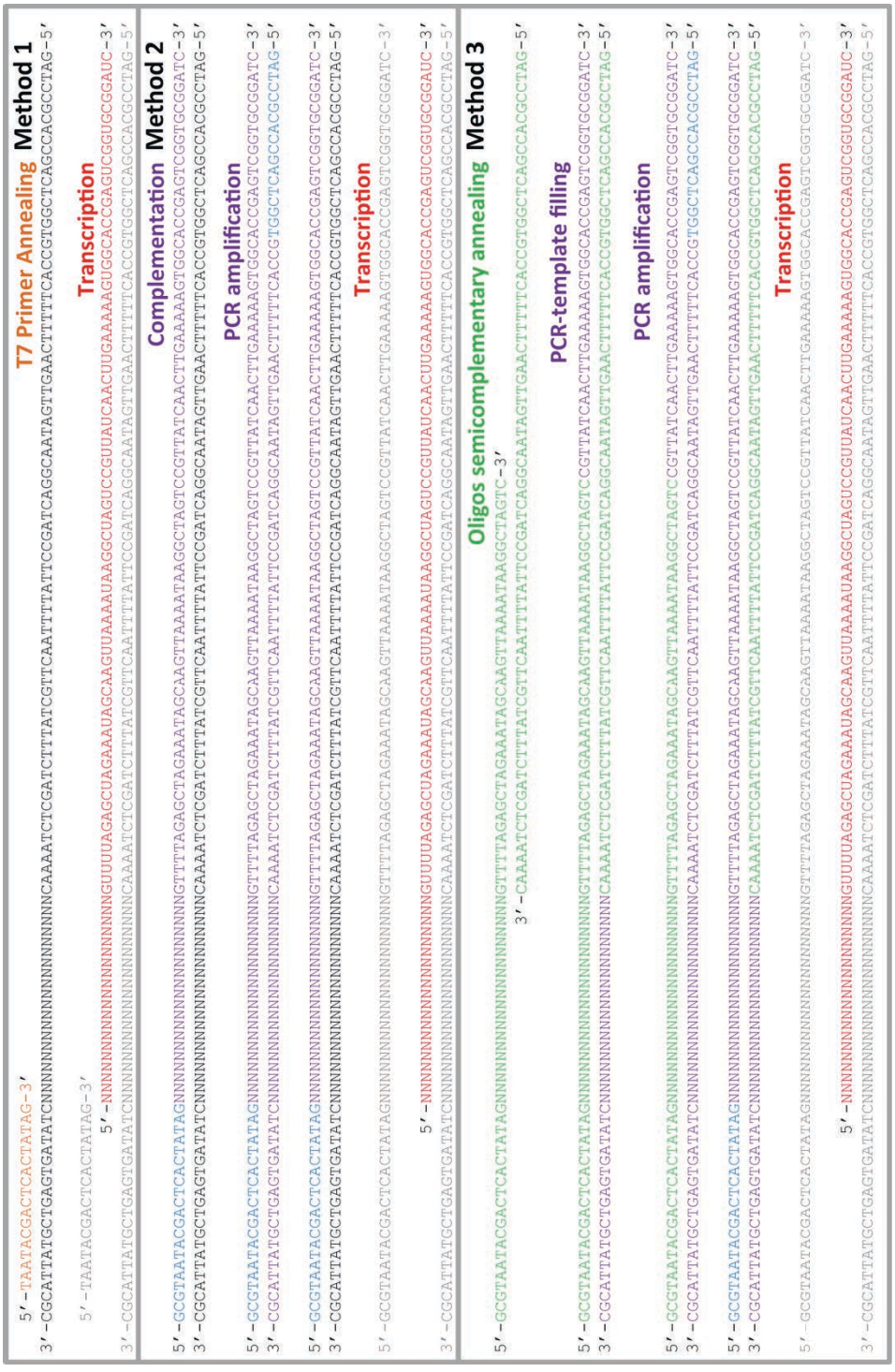

Figure 3. Methods for shgRNA transcription used in this study *(Legend on the next page)*.

Figure 3. **Methods for shgRNA transcription used in this study** *(Figure on the previous page).* Method 1 uses a synthetic 122-bases ssDNA oligonucleotide (purified by PAGE, black), annealed to a T7 primer (orange) as a direct template for RNA transcription. Method 2 uses a dsDNA template derived from a PCR-based complementation and amplification (violet) of the 122-bases synthetic ssDNA oligonucleotide (as in Method 1). Method 3 uses a dsDNA template derived from PCR-based complementation and amplification (violet) of 2 half-length partially complementary oligonucleotides (81-bases each, purification by standard desalting method, green).

Of note, the 81-mer oligo can be synthesised and purified by standard methods used to synthesise custom-made primers. The use of a PCR-based shgRNA template described here eliminates completely laborious cloning steps and permits to obtain a working shgRNA within 7-9 hours from the receipt of the 81-mer primer, while a cloning-based method would require at least 5 working days, since several O/N steps are required (**Table 3**)[55].

PCR-based shgRNA synthesis		Cloning-based shgRNA synthesis	
Ordering			
Day 1	1. Order 1 81-mer per shgRNA + a set of 3 constant primers (**1-2 days**)	**Day 1**	1. Order 2 primers per shgRNA + 1 constant receiving plasmid (**1-2 days**)
Generation of shgRNA template			
Day 2	2. PCR reaction (**2 h**) 3. Gel electrophoresis (**0.5 h**) 4. Column PCR cleanup (**0.5 h**) 3. Validation by sequencing (**O/N**) **Note**: All the templates can be made using a universal synthetic strategy.	**Day 2-3-4-5**	2. Primer annealing (**1 h**) 3. Plasmid digestion (**2 h**) 4. Ligation (**> 4 h**) 5. Transformation (**3 h**) 6. Plating + colonies forming (**O/N**) 7. Liquid culture (**O/N**) 8 Plasmid isolation (**1 h**) 9. Gel electrophoresis (**0.5 h**) 9. Validation by sequencing (**O/N**) 10. Plasmid linearisation (**2 h**) 11. Linear plasmid cleanup (**1 h**) **Note**: Not all the templates can be cloned using a universal cloning strategy.
shgRNA Transcription			
Day 3	4. *In vitro* transcription (**3-5 h**) 5. RNA cleanup (**1 h**) **Note**: PCR-based templates are transcribed with high efficiency (no risk of endotoxins, reduced amount of template, reduced likelihood of contamination with RNases).	**Day 6**	12. *In vitro* transcription (**3-5 h**) 13. RNA cleanup (**1 h**) **Note**: plasmid templates are transcribed with a reduced efficiency (chance of residual endotoxins, large amount of non-template DNA that can inhibit the reaction, more likely contamination with RNases).
Additional materials: DNA polymerase, PCR buffer + dNTPs.		**Additional materials:** Restriction enzyme, restriction buffer, ligase, ligation buffer + ATP, liquid and solid culturing media + antibiotics.	
Critical steps: RNA *in vitro* transcription.		**Critical steps:** primer annealing, ligation, transformation, clone selection and RNA *in vitro* transcription.	

Table 3. Comparison of the PCR-based shgRNA synthesis method used here with cloning strategies used elsewhere.

Method validation and RNA concentration titration for efficient targeting *in vivo*

To validate our method of shgRNA synthesis and to confirm the activity of the Cas9 mRNA, we co-injected the Cas9 mRNA with a shgRNA targeting eGFP in fertilised eggs of homozygote *Tg(fli1a-eGFP)*[45], a well-characterised zebrafish transgenic line where GFP is expressed by the endothelium of lymphatic and blood vessels[45]. We adapted to our synthetic strategy (Method 2) a published eGFP CRISPR target site which was already successfully used to suppress eGFP signal in a zebrafish transgenic line[15]. To assess the dependency of the targeting efficiency from the mRNA concentration and to assess general toxicity effects, a gradient of Cas9 mRNA and eGFP-shgRNA were injected ranging between 150 and 300 pg for the Cas9 mRNA and between 25 and 250 pg for the eGFP-shgRNA. Embryos were visualised under the fluorescent microscope at 30 and 48 hpf to screen for eGFP signal. Depending on the signal, the embryos were categorised into 3 groups: normal eGFP signal, mosaic eGFP expression or severe/complete abrogation of eGFP expression (**Figure 4A-D**). The combination of the highest doses (300 pg for Cas9 mRNA and 250 pg for eGFP-shgRNA) yielded the most effective targeting and resulted in the complete or almost complete loss of eGFP in about 20% of the *Tg(fli1a-eGFP)* and in a mosaic phenotype in 30% of embryos. The rest of the injected embryos maintained an apparent homogeneous eGFP expression, although the vast majority of them showed to some extent a reduced signal intensity when compared to the uninjected *Tg(fli1a-eGFP)* controls. It must be emphasised here that injections were performed in eggs which were homozygote for the *fli1a-eGFP* transgene, meaning that complete and mosaic loss of eGFP is derived from biallelic targeting in the whole organism or in a proportion of the cells. This experiment, therefore, demonstrates high efficiency of our PCR-based method for CRISPR-targeting.

Detection of CRISPR/Cas9 mutagenesis and efficiency

Next, we aimed to choose a screening methodology to validate active CRISPR targeting of genes such as *cxcr3.3* for which we did not expect a direct phenotypic targeting evidence. Several reports identify a T7 Endonuclease I (T7EI) assay as a screening methodology[15,16]. T7EI assay detects the presence of heteroduplex DNA (dsDNA carrying one or more mismatches), which is a result of the denaturation and renaturation of PCR amplicons derived from chimeric and/or heterozygote individuals. T7EI specifically digests heteroduplex DNA (e.g. derived from genome editing), by introducing double-strand breaks, whilst it does not digest homoduplex DNA (e.g. derived from uninjected controls). As a result, upon incubation with T7EI, the PCR product from individuals carrying mutations will be digested and will form multiple bands on agarose gels, whilst amplicons derived from wt embryos will appear unaffected and display a single band on gel. Detection of eGFP disruption could be achieved with this method (not shown); however, we have experienced poor robustness and reproducibility, since, in several cases, embryos with a complete loss of eGFP signal (and validated as disrupted eGFP individuals by Sanger sequencing) were indistinguishable from the uninjected embryos. At the end of a PCR reaction, all the DNA is in a homoduplex form. To permit formation of heteroduplex DNA, a specific protocol of denaturation-renaturation has to be performed (https://www.neb.com/protocols/2014/08/11/determining-genome-targeting-efficiency-using-t7-endonuclease-i). As a consequence, this method requires specific thermocycling conditions respecting precise timings and temperature gradients, which to some extent are also dependent on each specific PCR template (e.g. GC content, amplicon length etc.) and

should be fine-tuned empirically per each amplicon for optimal results. Therefore, we preferred screening of targeting by Sanger sequencing as a genotyping strategy.

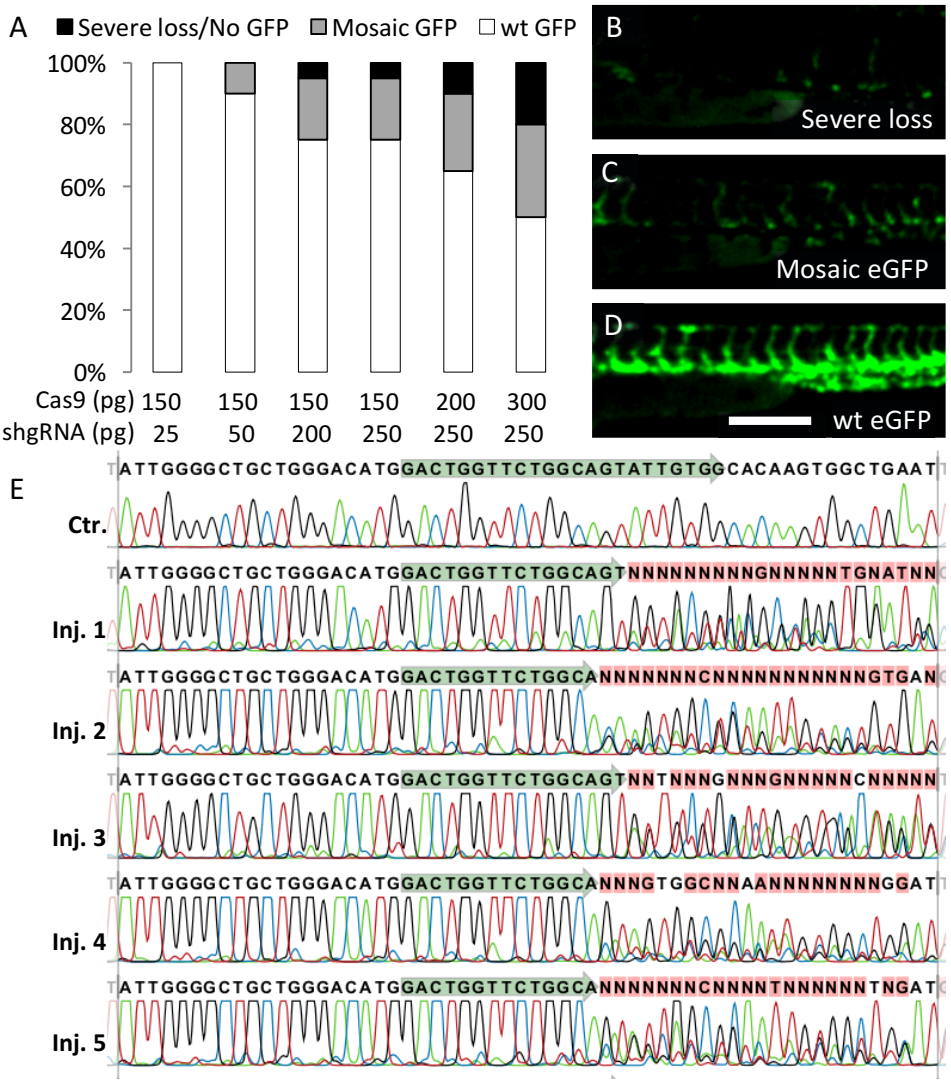

Figure 4. Efficiency of shgRNA/Cas9 mRNA injections. A-D. Effects of different concentrations of shgRNA/Cas9 RNA on the efficiency of eGFP CRISPR targeting. *Tg(Fli1a:eGFP)* embryos were injected with the indicated amounts of eGFP CRISPR shgRNA and Cas9 mRNA. In A, injected embryos were classified at 48 hpf based on the eGFP expression pattern. Increase of Cas9 and shgRNA correlated with increase of more severe phenotypes. B-D show representative images of eGFP-CRISPR injected fish, with different levels of GFP loss. **E.** Determination of *cxcr3.3* Target C sequence disruption by Sanger sequencing. CRISPR-injected fish exhibit sequence alterations (multiple peaks) downstream of the CRISPR target site (green label).

Comparing a wt and a mutated sequence by Sanger sequencing, one should observe a read composed of single peaks for the wt (indicating existence of only one base at each position in the amplicon), whilst a mutant sequence will be composed of single peaks upstream of the mutation point and by distorted multi-peaked reads from that point beyond, due to insertions and deletions of bases and to the simultaneous presence of wt and mutated reads (**Figure 4E**).

Of note, from our experience CRISPR mosaics display more than two alternative reads, indicating the concurrent occurrence of several mutations (**Figure 4-5**). Most likely this is due either to a) biallelic editing, leading to alternative mutations of the two genetic alleles, b) alternative repair mechanisms occurring in the forward and reverse strand of the genomic DNA, c) alternative mechanisms of repair taking place in daughter cells, or d) delayed CRISPR editing, occurring independently in individual daughter cells at more than 1-cell stage. Despite the fact that Sanger sequencing is required to confirm efficient targeting, we also found, in agreement with other laboratories, that long runs (>1h) on high percentage agarose gels (4%) permits detection of effective targeting in most of the samples where genome editing occurs. When compared to wt, amplifications derived from successful editing, do not appear as a sharp narrow band, but as a smeared band around the expected molecular weight (most commonly slightly higher). Of note, if electrophoresis is run for shorter times and/or on lower % agarose gels, mutant bands most commonly appear indistinguishable from wt.

Generation of a CRISPR/Cas9 mutant for *cxcr3.3*

ShgRNAs against the 4 target sites for *cxcr3.3* were injected at concentrations ranging between 30 and 150 pg along with 150 pg of Cas9mRNA. However, among the 4 selected targets, only one (Target C) displayed clear and efficient genome editing. When injected at the highest concentration, this shgRNA yielded an average efficiency per injection session of 70±17% as assessed via Sanger sequencing (**Figure 4E**). The other three targets consistently failed in generating mutations at the target site and were therefore discontinued. Over 200 eggs were injected with *cxcr3.3* Target C and raised to adulthood (F0). The offspring of 14 F0 adult fish (outcrossed to AB/TL) were genotyped. The results revealed that the final success rate of adult carriers was 71.4% (10/14). The tested carriers were able to transmit the mutated alleles with an efficiency of heterozygote F1 ranging between 17% and 100%, depending on the founder. The exact entity of the mutation carried by each heterozygote was determined by Sanger sequencing. By this method, heterozygotes display a double-peaked read from the mutated point onwards. By subtracting the wt sequence from the double-peaked read we could, therefore, obtain the read relative to the mutant allele (**Figure 5A**). This method proved very efficient for the selection of desirable mutations and of isogenic heterozygote carriers to generate full homozygote mutants by incross (**Figure 5B-E**). Our heterozygote sequence analysis also demonstrated that single F0 founders, when crossed to wt, could generate heterozygote offspring carrying different kinds of mutant alleles (**Figure 5E**). In particular, 4/10 founders generated offspring with more than 1 mutated allele and 3/10 transmitted more than 2 and up to 4 mutant alleles, indicating that the mechanisms of alternative repair and/or delayed targeting also contributed to the generation of alternative mutations, together with the biallelic targeting (**Figure 5E**).

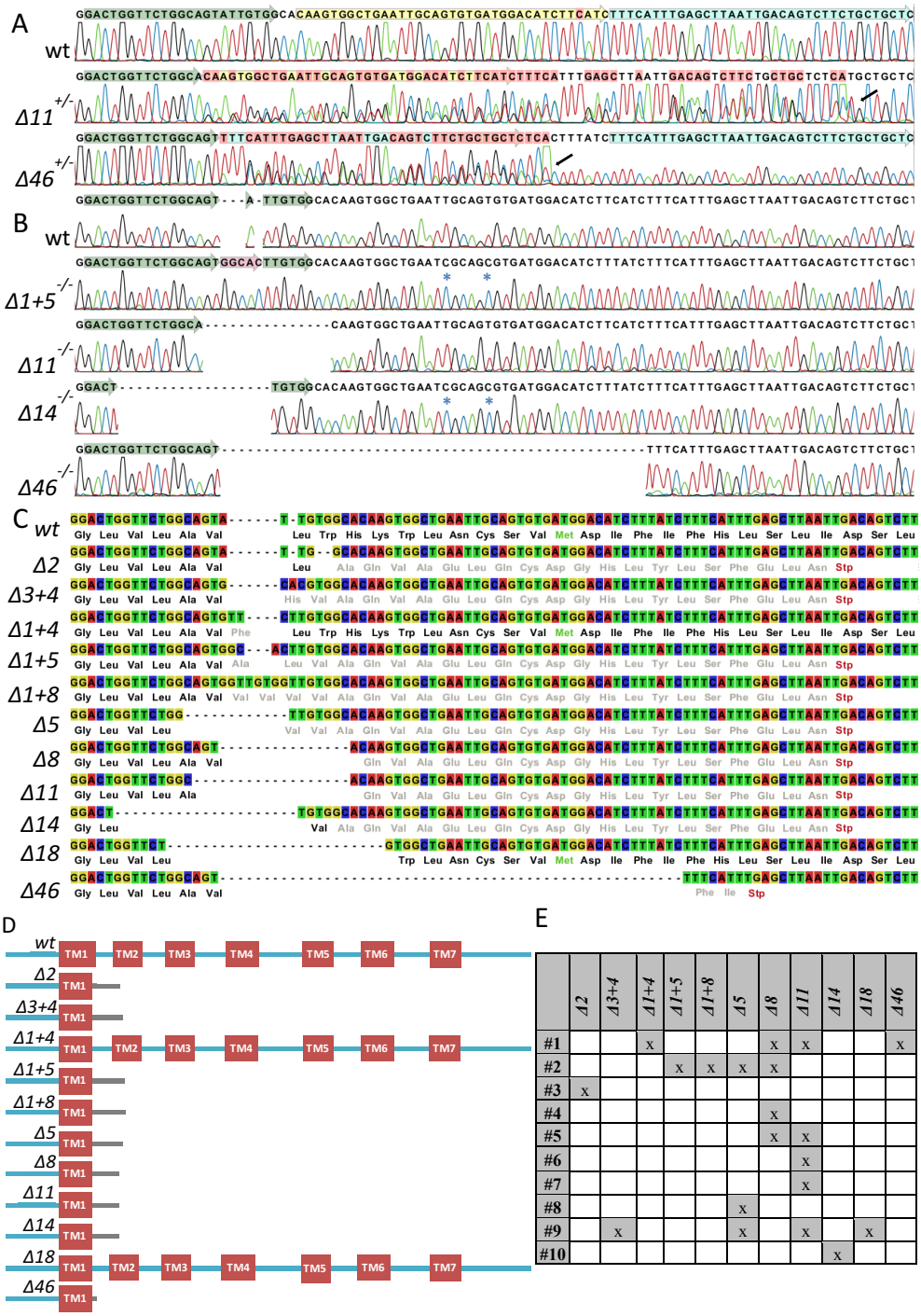

Figure 5. Identification and selection of *cxcr3.3* mutations *(Legend on the next page)*.

Figure 5. Identification and selection of *cxcr3.3* mutations *(Figure on the previous page)*. **A.** Double-peaked reads of heterozygote carriers. When compared to wt, heterozygote mutant carriers display double peaks from the start of the mutation sequence onwards. At each nucleotide position, the double read is due to the nucleotide read of the wt allele and the nucleotide read of the mutant allele, meaning that the mutation type can be identified by subtracting the wt sequence from the double-peaked read. Mutant *Δ11* displays a wt-subtracted read that matches the wt sequence 11 nucleotides downstream the start of the mutation (yellow label), indicating that the mutant carrying this alteration has a deletion of 11 nucleotides. Mutant *Δ46* displays a wt-subtracted read that matches the wt sequence 46 nucleotides downstream the start of the mutation (blue label), indicating that the mutant carrying this alteration has a deletion of 46 nucleotides. Black arrows at the end of the mutant sequences indicate where the shorter mutant allele sequence has terminated, due to the end of the amplicon. Upon this position only the longer wt sequence is read, therefore, the sequence appears again single-peaked. **B.** Sequence alignment of confirmed homozygote mutants, generated from incross of heterozygote carriers of the same mutation. Blue asterisks indicate nucleotides that are naturally polymorphic in the wt population. **C-D.** Alignment of all identified mutations and their consequence at protein level. In D, red boxes indicate the predicted transmembrane helices, regions in grey indicate sequences that diverge from the wt sequence (translation of inserted nucleotides and of frame-shifted coding sequences). Notably *Δ1+4* and *Δ18* mutations would lead to in-frame mutant variants, with 3 additional amino acids or 6 deleted amino acids at the end of the TM1 domain, respectively. All the other mutations would generate frameshifts and premature protein truncation. **E.** Analysis of the offspring of 10 *cxcr3.3* F0 founders (#1-#10). Several F0 can transfer multiple kinds of mutations to their offspring (crosses), indicating that biallelic targeting and alternative mechanisms of damage repair/delayed targeting contribute to the generation of alternative mutant alleles. Data also show that some individual founders carry identical mutations, suggesting that preferred types of mutations are mediated by CRISPR/Cas9 targeting.

The profile of the F1 generation from different founders also suggested that preferred mutations may occur. For example, specific mutations (*Δ5*, *Δ8* and *Δ11*) occurred in more independent founders (3/10, 4/10 and 5/10 respectively). Additionally, 6/10 independent founders carried at least one large (>10 dNTPs) mutation, which are particularly useful to permit a simple procedure for genotyping by PCR and gel electrophoresis.

Mutation of *cxcr3.3* does not alter development and survival of homozygote mutants, but affects *M. marinum* infection burden

Among the identified mutations we selected the non-sense *cxcr3.3Δ46* and the *cxcr3.3Δ11* alleles to further investigate the function of *cxcr3.3*. These mutations were chosen since they were transmitted with high frequency from the F0 founder to its heterozygote offspring, which enabled to timely obtain sufficiently-sized and properly mating isogenic families. Additionally, since these mutations consist of > 10 bp deletions, genotypes could be distinguished using PCR and gel electrophoresis. Heterozygote carriers of *cxcr3.3Δ46* and of *cxcr3.3Δ11* mutations were incrossed with isogenic mutation carriers to obtain homozygote mutant, heterozygote and homozygote wt offspring, which was raised to adulthood as mixed families. We found that in both families *cxcr3.3* mutants maintained Mendelian proportions with the other genotypes, therefore we concluded that *cxcr3.3* mutation is viable and does not confer a major disadvantage to the carriers (**Figure 6A-B**). Phenotypic inspection of embryos and larvae also did not reveal any significant developmental differences between mutant and wt siblings. Adult homozygote mutants were fertile and could produce viable offspring. To address whether *cxcr3.3* may have a function in controlling the immune response, we injected mutant and wt (either derived from heterozygote incross or from homozygote mutant and wt siblings incrosses) at 1 dpf with the fish pathogen *Mycobacterium marinum* (*Mm*). At 4 dpi both *cxcr3.3Δ46* and *cxcr3.3Δ11* mutant larvae displayed a significantly higher infection burden than their wt

counterparts, indicating that *cxcr3.3* mutation is detrimental to combat mycobacterial infection (**Figure 6C-F**). This phenotype is opposite to that previously described for a *cxcr3.2* mutant, which shows an attenuated formation of granulomatous lesions and increased resistance to *Mm* infection[9]. In view of the opposing infection phenotypes of these two receptor mutants, we analysed the infection burden evoked by *Mm* in larvae exposed to NBI74330, an antagonist of CXCR3 that, based on binding pocket similarity should inhibit both Cxcr3.2 and Cxcr3.3 in zebrafish (**Figure 6F-G**). Treatment with this compound revealed a *cxcr3.2* mutant-like phenotype and a reduction of mycobacterial infection burden (**Figure 6H**).

Cxcr3.3 in zebrafish and other teleosts displays sequence features common to atypical chemokine receptors

While further in-depth characterisation of *cxcr3.3* mutants is still necessary to fully understand the function of the Cxcr3.3 receptor and its crosstalk with Cxcr3.2, we used computational sequence analysis to examine whether the opposing functions of these receptors in controlling mycobacterial infection could have a structural basis. We found that, when compared to human CXCR3 and zebrafish Cxcr3.1 and Cxcr3.2, Cxcr3.3 displays specific amino acid substitutions. In particular, the DRY sequence (Asp-Arg-Tyr), an extremely conserved motif that permits coupling of the chemokine receptors to the heterotrimeric G-proteins, contains an R (Arg) to C (Cys) replacement (**Figure 7**, **Supplementary Figure 1**)[56].

The R of the DRY motif is the most conserved residue of functional G-coupling GPCRs and presents 100% conservation among typical human CXC receptors (CXCR1-2-3-4-5-6-8). Replacement of this residue is known to abolish transduction of heterotrimeric G-protein signalling in chemokine receptors[57], as this amino acid is believed to interact directly with the G subunits to catalyse GDP release and therefore serves as an effector for G-protein activation[58,59]. Alteration of the DRY consensus is recurrent in atypical chemokine receptors (ACKRs; > 71% of the cases in humans) and in related GPCRs, such as viral GPCR-like seven transmembrane proteins or atypical anaphylotoxin receptors. Examples in humans are DARC/ACKR1 (DRY to GHR), D6/ACKR2 (DRY to DKY), CCRL2/ACKR5 (DRY to QRY), PITPNM3/ACKR6 (DRY to SSR) and C5L2 (DRY to DLC, a decoy interceptor for the anaphylotoxin C5a). Exceptions are represented by CXCR7/ACKR3 and CCRL1/ACKR4, whose DRY sequences are not divergent, and in which failure of G-protein activation is most likely due to the replacement of other residues of the so-called micro-switch elements that permit transition of the GPCR from the inactive to the active form[60,61]. Notably, several replacements in the micro-switch elements are present also specifically in Cxcr3.3, when compared to its human and zebrafish orthologues (**Figure 7**).

To further dissect whether the existence of an atypical Cxcr3 is an exclusive prerogative of zebrafish, we analysed the sequence of the CXCR3 proteins derived from 19 vertebrate genomes (11 fish, 1 amphibian, 2 reptiles, and 5 mammals). We found that, while in tetrapods the R residue of CXCR3 is 100% conserved, in 82% of the fish species analysed here at least one Cxcr3 isoform displays an R residue substitution.

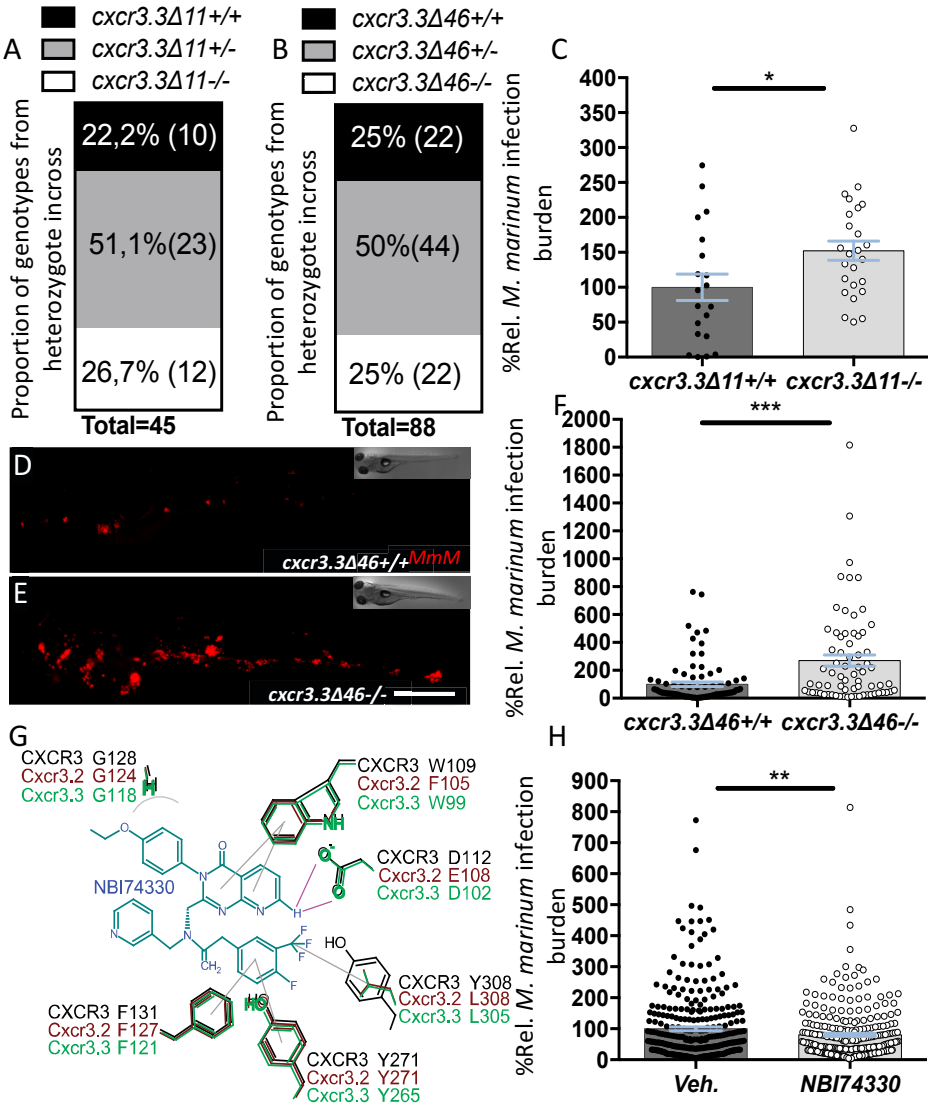

Figure 6. Characterisation of *cxcr3.3* mutants. A-B. Mendelian segregation of *cxcr3.3Δ46* and *cxcr3.3Δ11* mutant alleles. Families derived from incross of heterozygote carriers for one or the other mutation did not display deviation from Mendelian genotype ratios at the sexually mature age, indicating that *cxcr3.3* mutant alleles do not affect survival. **C-F.** Quantification (% relative to wt) of *Mm* infection burden at 4 dpi in *cxcr3.3Δ11* (C) and *cxcr3.3Δ46* (F) mutant and wt siblings. 28-30 hpf embryos were infected with 100-200 CFU of *Mm*. Representative pictures of infected wt and mutant larvae are shown in D-E**.** Data in C derive from 1 replicate. Data in F derive from three cumulated experiments. **G.** NBI74330 binding pocket of CXCR3, Cxcr3.2 and Cxcr3.3. Key amino acid residues are conserved, suggesting that this drug can antagonise both the human and the two zebrafish receptors. **H.** Quantification (% relative to vehicle DMSO, veh.) of *Mm* infection burden at 4 dpi in 25 µM NBI74330 and DMSO (Veh.)-treated group. 28-30 hpf embryos were infected with 200-250 CFU of *Mm*. Data are cumulative from three replicates. Treatment with NBI74330 mimics *cxcr3.2* phenotype and not *cxcr3.3* phenotype. Each data point in C, F, H represents a single individual. Error bars: mean±s.e.m. Scale bar: 500 µm.

Notably, as in the case of zebrafish Cxcr3.3, polymorphisms in the DRY sequence of Cxcr3 isoforms in other fish are also linked to the substitution of micro-switch elements (**Figure 8**). In one of the two fish species (Cod) where no DRY-altered isoforms are observed, several micro-switches are still present in one of the isoforms, which would, therefore, suggest that in this organism one of the Cxcr3 isoforms is also atypical (**Figure 8**). It must be noted that two tetrapod sequences also displayed alteration of the DRY sequence, although not of the R residue. (DRY to ERY and DRY to NRY). Synonymous D/E change (present in the anole lizard Cxcr3.2) is frequently observed in other GPCRs and is generally not thought to alter G-protein signal transduction[58].

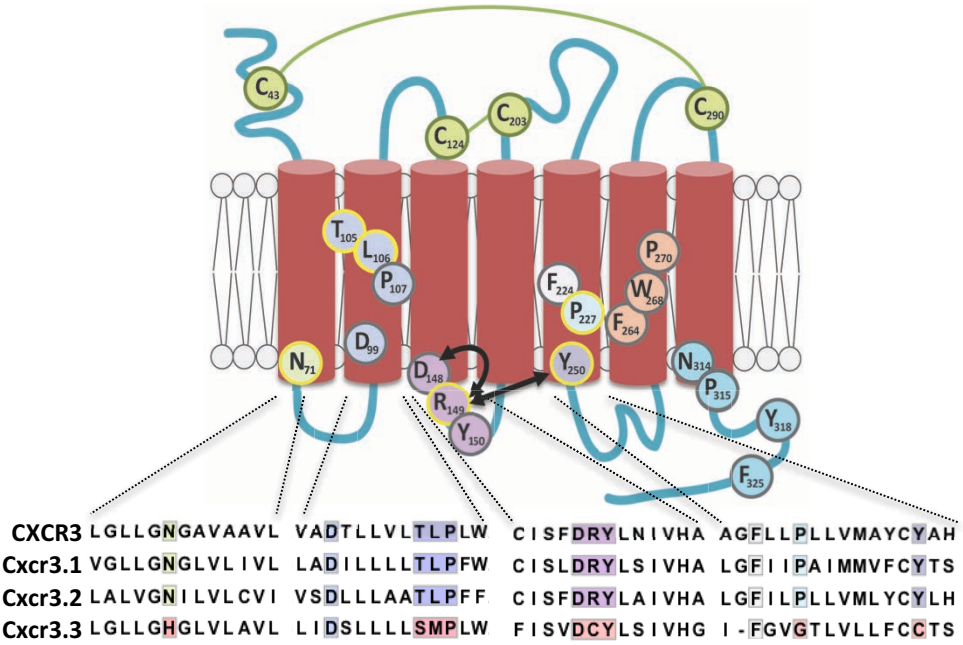

Figure 7. Cxcr3.3 displays replacement of several amino acids fundamental to G-protein-dependent signal transduction. Compared to its zebrafish homologues, Cxcr3.3 has several sequence alterations which suggest it might function as an atypical chemokine receptor. The TLP sequence (105-107) is known to be important for stabilisation of micro-conformational switches to transduce signalling upon binding to the chemokine ligand and is replaced with SMP in Cxcr3.3. The DRY (148-150) sequence and the Y_{250} are fundamental for the interaction and activation of the G-proteins. In the inactive state, R_{149} interacts with D_{148}, while in the active conformation R_{149} interacts with Y_{250} and G-proteins. R_{149} represents the most conserved residue among active chemokine receptor and is changed to C in Cxcr3.3. Similarly, Y_{250} is also highly conserved and substituted with a C in Cxcr3.3. Virus-encoded 7TM receptors and most of ACKRs, such as ACKR1-2-5, have altered DRY motifs, explaining their inability to mount classic chemotactic signals and their altered biological activities. Notably, Cxcr3.3 has also a replacement of N_{71} and P_{227} with H and G respectively. In chemokine receptors from different species these two residues represent the most conserved residues of TM1 and TM5, respectively, and they possibly also exert important functional roles in conformational changes and signal transduction. Amino acids circled in yellow are key residues that are specifically substituted in Cxcr3.3 when compared to its human and zebrafish homologues. Subscript positional numbers of the amino acid residues represent the progressive numeration of residues according to the human canonical CXCR3 isoform.

The non-conservative D/N replacement (present in xenopus Cxcr3.2) has been reported to abrogate chemokine signalling in some studies on other receptors[62]. However, no other micro-switch substitutions were associated with this Cxcr3 isoform, which therefore is most likely phylogenetically homologous to the typical Cxcr3 receptors. Overall, our study suggests that early in teleost evolution an alternative atypical *cxcr3* gene evolved, a feature that is currently maintained in a variety of modern fish species, but lost during the radiation of higher vertebrates.

Based on the fact that Cxcr3.3 receptors has an evolutionarily conserved alteration of the DRY motif and of regulative micro-switch elements, we propose that this receptor may antagonise the canonical Cxcr3 isoforms by competing for ligands. Changes in the DRY and in micro-switches do not generally alter the ligand binding domains and their capability to efficiently bind ligands. However, the expression of this atypical isoform may, in turn, reduce the possibility for Cxcl11 ligands to bind and signal via their classical receptors, therefore modulating the levels of signals evoked in the stimulated cells. In the context of mycobacterial infection, where depletion of canonical signalling via Cxcr3.2 is beneficial to the host, depletion of *cxcr3.3* could translate instead into an exuberant exploitation of Cxcr3.2 signalling with, in turn, detrimental effects on the host.

DISCUSSION

By using *cxcr3.3* targeting as a case study, we have set up a simple and fast protocol for efficient CRISPR/Cas9 mutagenesis in zebrafish (**Graphical protocol**). This method uses the synthesis of a dsDNA template by annealing, PCR filling and amplification of two semi-complementary 81-mer oligonucleotides. This DNA amplicon serves as a template for the shgRNA *in vitro* transcription. Upon transcription of the shgRNA and of a zebrafish-optimised NLS-Cas9-NLS mRNA, the two components can be coinjected into zebrafish embryos at the 1-cell stage. Target efficiency can be detected by Sanger sequencing of injected individuals, according to the emergence of secondary reads in the electropherogram within the target site. ShgRNAs that do not yield high targeting efficiency can be discontinued, while highly efficient targets can be injected in a larger egg batch for culturing. The selected target that we used to obtain *cxcr3.3* mutants, yielded over 70% efficiency in adult germ-line transmitted gene editing and required screening of as few as 10 F0 positive individuals to identify several large (> 10 dNTPs) mutations, which allowed easy detection of genotypes by PCR and gel electrophoresis. From the analysis of the F1 generations we found that our targeting method led to biallelic editing and that other mechanisms of independent attempts of repair/delayed targeting also contributed to the generation of alternative genome modifications. This translated into a high percentage (40%) of F0 founders carrying more than one mutation in their germ-line.

The high yield and the biallelic targeting of this strategy also imply that this approach might be explored as an alternative to morpholino-based transient knockdown, with the advantages that CRISPR/Cas9 constructs are more affordable in terms of costs, do not evoke morpholino-dependent toxicity phenotypes, and their targeting leads to stable gene mutations which denotes that their effect would not reduce in time by dilution and degradation.

Figure 8. Atypical Cxcr3 isoforms are recurrent in fish. Alignment of CXCR3 proteins in vertebrates. Most of the fish species analysed have at least 3 copies of CXCR3. With the exception of cod (gmo) and tetraodon (tni), the other species have at least one isoform where the DRY sequence has been modified in the conserved R_{149} residue. In most species, Cxcr3.3 presents also a replacement of the conserved Y_{250}, C_{290} and N_{314} residues. Y_{250} interacts with R_{149} during receptor coupling with the G-proteins. Therefore, it is likely that also in cod the Cxcr3.3 isoform, despite the DRY consensus, is unable to function due to Y_{250} replacement. In spotted gar (loc), only a DRY-disrupted Cxcr3.3 isoform is currently known. However, a functional Cxcr3 could exist in this species and might remain unidentified due to poor quality of the genome sequence in the *cxcr3* locus[63]. Amphibians and reptiles have one or two copies of CXCR3. In xenopus (xtr) and the anole lizard (aca), the DRY sequences of one of the two isoforms have been modified into NRY and ERY, respectively. These changes are predicted to impact less severely on the receptor coupling to G-proteins. Additionally Y_{250}, C_{290} and N_{314} remain conserved, suggesting that these isoforms may be functional and non-homologous to fish Cxcr3.3. In mammals, *CXCR3* is present as a single classical isoform. Legend: aca: *Anolis carolinensis* (anole lizard); ame: *Astyanax mexicanus (*cave fish); bta: *Bos taurus* (cow); dre: *Danio rerio* (zebrafish); gac: *Gasterosteus aculeatus* (stickleback); gmo: *Gadus morhua (*cod); hsa: *Homo sapiens* (human); laf: *Loxodonta africana* (elephant); loc: *Lepisosteus oculatus (*spotted gar); mus: *Mus musculus* (mouse); ola: *Oryzias latipes* (medaka); oni: *Oreochromis niloticus* (tilapia); psi: *Pelodiscus sinensis* (Chinese softshell turtle); pfo: *Poecilia formosa (*amazon molly); tni: *Tetraodon nigroviridis* (tetraodon); tru: *Takifugu rubripes* (fugu); xma: *Xiphophorus maculatus (*platyfish); sha: *Sarcophilus harrisii* (Tasmanian devil); xtr: *Xenopus tropicalis* (western clawed frog). Sequences were all obtained from Ensembl database.

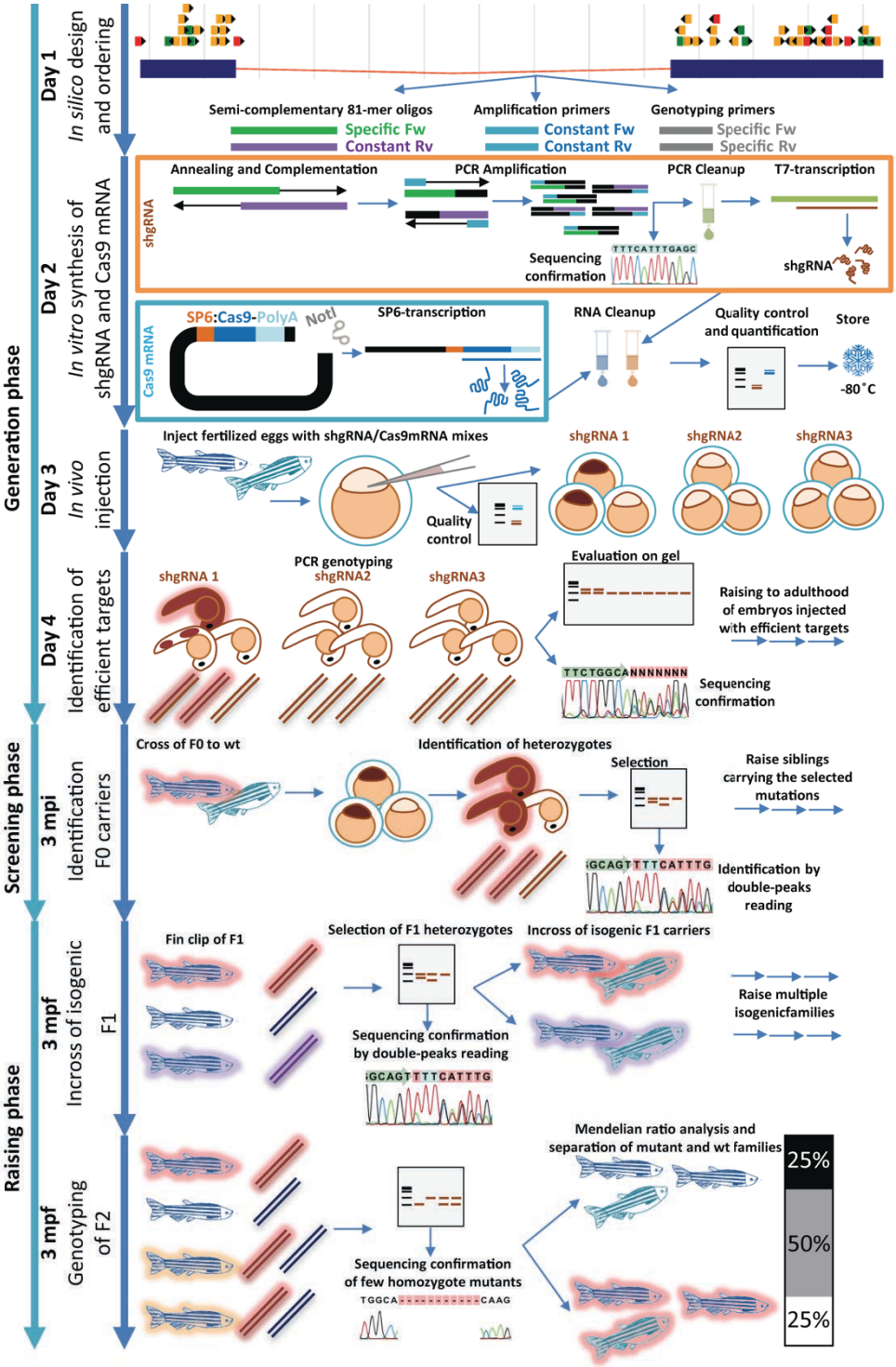

Graphical protocol *(Legend on the next page)*.

Graphical protocol *(Figure on the previous page)***.** The first phase to generate a CRISPR knockout zebrafish line consists in the *in silico* design and ordering of custom-made oligonucleotides, which will be used as a template to synthesise the shgRNA *in vitro* (81-mer semicomplementary oligomers and template amplification primers), or to genotype the animals via PCR and sequencing (genotyping primers). Different online tools are available to select suitable CRISPR targets and suitable genotyping primers. The left 81-mer oligonucleotide contains the T7 promoter sequence (necessary to initiate the RNA transcription once the template has been produced) followed by the CRISPR target sequence and part of the invariable sequence of the shgRNA. The right 81-mer oligonucleotide contains the complementary sequence to the terminal region of the left 81-mer and the remaining part that completes the invariable shgRNA sequence. The two oligos can anneal with each other and the shgRNA template can be filled by a few PCR cycles. To produce a quantitative amount of template, this product requires further PCR amplification using short constant primers that anneal to the termini of the product (T7 sequence and extremity of the invariable shgRNA sequence). Once the amplicon has been cleaned up and confirmed by sequencing, it can be used as a DNA template to produce the shgRNA. Simultaneously, also the Cas9 mRNA can be *in vitro* transcribed from a NotI-linearised plasmid template. The two mRNAs require column clean up, gel-electrophoresis and nanodrop quality control and quantification. Single-use aliquots of both RNAs can be stored for undefined time at -80°C. A mix of shgRNA and Cas9 mRNA can be injected into zebrafish fertilised eggs. Different shgRNA (shgRNA1, 2 and 3) may be injected side by side, to maximise the chance of identifying an efficient target site. From 24 hours post fertilisation, dechorionated embryos can be sacrificed for PCR genotyping, in order to verify successful genome editing and to estimate the targeting efficiency. The most efficient target can be injected on a larger scale to raise a family of potential founders (F0). F0 carriers can be screened as early as three months post injection (mpi), by single backcrosses to wt animals. The mutations will be transferred to part of the offspring in heterozygosis. Because the wt sequence is known, the exact mutations carried by each founder can be extrapolated from the double peak sequencing reads of their heterozygote offspring. The preferred mutations (e.g. large deletions generating a frameshift) can be selected for further characterisation. Since a single F0 founder has been shown to frequently transfer multiple mutated alleles to its offspring, it is likely that an F1 family will consist of a mixed population of animals carrying various mutations of the target gene. The different alleles can be distinguished by DNA extraction and genotyping from the fin clip. Isogenic founders can be pooled together to generate isogenic F1 families, carrying only one kind of mutation. Finally, at three months post fertilisation (mpf) these families (that consist exclusively of heterozygotes) can be incrossed to obtain homozygote mutants, wt and heterozygotes (F2). The ratio between the genotypes in F2 can be used to assess whether the mutation affects the survivability of the animals. Sibling families of homozygote mutants and wt can be kept as breeding colonies to collect embryos of known genotypes for experiments.

Using the CRISPR/Cas9 editing system we obtained several stable mutant lines of *cxcr3.3* and performed an initial characterisation of them. Under physiological conditions, we did not observe any advantage/disadvantage in carrying a *cxcr3.3* mutant allele, in either heterozygotes or homozygotes. However, we found that infected mutant individuals display an increased susceptibility to the pathogen *Mm*, which indicates an underlying function of Cxcr3.3 in the control of mycobacterial infection. We currently do not know the exact mechanisms by which Cxcr3.3 is required to respond to mycobacteria and further analysis is needed. Strikingly, the phenotype of this mutant in control of mycobacterial infection differs from that of the *cxcr3.2* mutants, which display a reduced susceptibility to the same pathogen[9]. A possible hypothesis, confirmed by structural predictions is that Cxcr3.2 and Cxcr3.3 antagonise each other by ligand competition and/or induction of alternative transduction signals. Several chemokine receptors have been shown to antagonise or synergise each other[64]. ACKRs, for example, are seven transmembrane receptors homologous to chemokine GPCRs that have a modified or missing canonical DRY motif within the second intracellular loop, which makes them unable to couple to G-proteins and induce the full spectrum of "classical" GPCR signalling and cellular

responses, including cell migration[65,66]. Several mechanisms by which ACKRs influence the responses to chemokines have been shown. D6/ACKR2, for example, is an ACKR for a wide array of CC chemokines. Upon binding to these ligands, the ligand-receptor complex is internalised and transferred to late endosomes. Here the ligands dissociate and are degraded by endolysosome maturation, while the receptor is recycled and re-expressed at the plasma membrane. This mechanism allows D6/ACKR2 to scavenge CC chemokines and reduce binding to their canonical G-protein coupled receptors[67].

CXCR7/ACKR3 is another member of the atypical chemokine receptor group, which cannot couple to G-proteins, despite still being able to bind β-arrestin and transmit MAPK-mediated signalling to some extent[60,64]. The zebrafish model has helped to elucidate the role of CXCR7 in the scavenging of CXCL12 ligand, thereby controlling the formation of a CXCL12 gradient which permits optimal migration. While binding of CXCL12 to CXCR4 transmits active chemokine signalling, binding of the same ligand to CXCR7 does not elicit G-coupled signal transduction. This translates into a reduced ligand binding to CXCR4 and therefore to an attenuated activation of the CXCR4-dependent cascade. This mechanism has been shown in zebrafish and mammals to finely control the direction of cell migration, as CXCR4 and CXCR7 are expressed with different expression dynamics and patterns (e.g. they mature and reside at the membrane with different timings)[6,68]. Additionally, similar to D6/ACKR2, CXCR7/ACKR3 sequesters CXCL12 and mediates its intracellular degradation[69].

Even "classical" chemokine receptors when simultaneously expressed may interfere with each other. Heterodimerisation of GPCRs is a well-known process. Several studies suggest that particular combinations may affect the receptor conformations and lead to dampened capability to bind ligands or to transduce signalling. Expression of chemokine receptors in absence of their ligands can also interfere with the signalling of other receptors whose ligands are present, when both are expressed by the same cell. Consuming/sequestering intracellular signalling molecules (e.g. β-arrestin or heterotrimeric G complexes, which are associated with resting receptors in unstimulated conditions) can in fact uncouple the antagonised receptor from its downstream signalling machinery[70].

Sequence alignment of zebrafish and human CXCR3 receptors indicates that the key DRY motif required to couple with heterotrimeric G-protein complexes is altered in Cxcr3.3, while Cxcr3.1 and Cxcr3.2 maintain an intact consensus sequence. Replacement of R with C in Cxcr3.3 suggests that this receptor belongs to the group of atypical chemokine receptors. In line with this theory it is possible that depletion of c*xcr3.3* would increase the availability of Cxcl11 ligands for Cxcr3.2, therefore inducing an enhanced (and detrimental for the host) Cxcr3.2-dependent signalling. Consistent with this hypothesis, the CXCR3 antagonist NBI74330, predicted to inhibit both Cxcr3.2 and Cxcr3.3, evokes an infection phenotype similar to that of *cxcr3.2* mutation, which means that Cxcr3.3 blockade cannot be detrimental if Cxcr3.2 signalling is also simultaneously depleted. That similar dynamics take place *in vivo* during mycobacterial infection is already indicated by a recent study on D6/ACKR2 knockout mice, which showed that these animals are more susceptible to mycobacterial infection, due to the increased number of monocyte/macrophages, DCs and T cells infiltrated in the lesioned tissues. Blockade of several chemokines with a combination of antibodies could rescue the phenotype of D6 deficiency, which suggests that the activity of D6/ACKR2 as a chemokine scavenger receptor is fundamental to maintain a balanced activation of leukocyte recruitment via the chemokine signalling[71].

Notably, interference with Cxcr3.2/Cxcr3.3 signalling might not act exclusively at the level of ligand-competition, since we also have previously found that *cxcr3.3* expression is controlled (at least in macrophages) by expression of *cxcr3.2*, as macrophages from *cxcr3.2*-deficienct larvae displayed a 1.5-fold decrease of *cxcr3.3* expression too[40]. This is particularly intriguing considering that not only did *cxcr3.2* control *cxcr3.3*, but also several genes for Cxcl11 ligands (Cxcl11aa-af-ag), whose expression in macrophages was 2-to-3-fold reduced in *cxcr3.2* mutants[40]. Functional signal transduction assays for Cxcr3.3 and analysis of *cxcr3.2-cxcr3.3* double mutant phenotypes will help to understand the exact interactions at play between these two paralogues.

It is noteworthy that, besides modifications in structural motifs required for G-protein activation, the preferential cellular expression and/or intracellular localisation may represent another aspect of Cxcr3.2/Cxcr3.3 biology contributing to their ability to activate G-protein-dependent signalling. Regarding cell specificity, both genes are expressed in macrophages and neutrophils. However, *cxcr3.2* is expressed more predominantly by macrophages, while *cxcr3.3* is more highly expressed by neutrophils[9]. This may result in a differential (cell-specific) ratio of receptor copies available for ligand binding in the two cell subsets. This may also explain why *cxcr3.2* mutation, despite the gene being expressed by both macrophages and neutrophils, displayed predominantly a macrophage phenotype rather than an effect on neutrophils. Injection of Cxcl11aa-af ligands, for example, could elicit significant macrophage recruitment, while neutrophil chemoattraction was comparable to mock-injected individuals[9]. This observation might indicate that the scavenging activity exerted by Cxcr3.3 in neutrophils reflects weak activation of G-protein signalling by Cxcl11 ligands in these cells, insufficient to support cell migration. In contrast, predominant expression of *cxcr3.2* over *cxcr3.3* in macrophages might permit sufficient active signal to sustain chemotaxis. Taken together, the generation and characterisation of the zebrafish *cxcr3.3* mutant line has provided more information on the translational utility of this model for biomedical research. Furthermore, it may also shed light on the evolution of typical and atypical chemokine receptors and on the selective forces acting on the immune system genes that, by duplication and functional specialisation, permitted the evolution of complex regulative mechanisms to tightly control biological processes.

MATERIAL AND METHODS

Synthesis of shgRNA – Primers and oligos up to 81 nucleotides were obtained from Sigma-Aldrich, using standard synthetic procedures (25 nmol synthesis scale, purification via desalting method). The 122-base template oligonucleotides were ordered from Integrated DNA Technologies (1 nmol synthesis scale, purification via PAGE Ultramer method), since the nucleotide length exceeds the maximum sequence length supported by Sigma-Aldrich and standard synthetic procedures. Sequences are reported in **Supplementary Table 1**. DNA template synthesis for the three methods described above was performed as follows.

In Method 1, the 122-mer oligos and the T7 promoter primer were suspended in TES buffer (10 mM Tris-HCl, pH=8, 1 mM EDTA, 0.1 M NaCl) to a 100 μM concentration. Before *in vitro* transcription, an equimolar amount (1:1 volumes, 50 μM each) of the 122-base oligo and of the T7 promoter primer were mixed. Annealing was obtained by

transferring the solution to a 95^{o}C water bath. After 1 min, the bath was switched off and let cool down to room temperature (about 30 minutes). The annealed mixture was then transferred to ice, diluted 10x with RNAse-free water and used as a template for *in vitro* transcription.

In Method 2, the 122-mer oligos were suspended as in Method 1 (100 µM in TES buffer) and 1 ng was used as a template in a PCR reaction (50 µl reaction, 200 µM dNTPs, 1 unit DreamTaq polymerase (Thermo Fisher Scientific), initial denaturation 95^{o}C/3 min 35 amplification cycles 95^{o}C/30 s, 55^{o}C/60 s, 72^{o}C/30 s, final extension step 72^{o}C/15 min), using template amplification primers as reported in **Supplementary Table 1** (0.5 µM each). The PCR product was column-purified using a PCR clean-up combo kit (Invitrogen), eluting the product in 20 µl of RNase-free water, and the expected size was checked by gel electrophoresis.

In Method 3, semi-complementary 81-mer oligo pairs (0.04 µM each) were annealed together and the product was completed by a short PCR program (50 µl reaction, 200 µM dNTPs, 1 unit DreamTaq polymerase, initial denaturation 95^{o}C/3 min, 5 amplification cycles 95^{o}C/30 s, 55^{o}C/60 s, 72^{o}C/60 s, final extension step 72^{o}C/15 min). The mix was removed from the thermocycler, maintained at room temperature, supplemented with template amplification primers as in Method 2 (0.5 µM each), and then returned to the thermocycler for further amplification (initial denaturation 95 ^{o}C/3 min, amplification 35 cycles 95^{o}C/30 s, 55^{o}C/60 s, 72^{o}C/30 s, final extension step 72^{o}C/15 min). The product was then purified by column clean-up as in Method 2. When running the PCR reaction using only one 81-mer oligo as a negative control we have frequently observed amplification at comparable size of the expected product of a complete reaction. This was most likely due to the existence of self-complementary stretches in the oligos. However, secondary reactions did not occur when both oligos were provided, as demonstrated by Sanger sequencing of the amplicons.

***In vitro* transcription of shgRNA** – For *in vitro* transcription of shgRNA, we used the MEGAshortscript T7 kit (Invitrogen) and 2530 fmols of template DNA (corresponding to 100 ng of ssDNA annealed to T7 primer for Method 1 and to 200 ng of PCR-derived dsDNA for Method 2 and 3). Purification of the shgRNA was achieved using the miRNeasy isolation kit (Qiagen) according to manufacturer's guidelines and eluting 2x10 µl in RNase-free water. Efficiencies for each method are reported in **Table 2**. Concentration was measured by nanodrop and integrity was checked by non-denaturing 2% gel electrophoresis and RNA-chip (RNA 6000 Pico kit, Agilent technologies) on 2100 Expert bioanalyzer (Agilent Technologies). The shgRNA may appear on the non-denaturing gel as a single or double band, depending on temperature and on how delayed the running of the gel is from the column elution. When maintained at room temperature the shgRNA formed two bands, with a more intense one at lower molecular weight. If the RNA was warmed to > 55^{o}C and immediately loaded, it appeared as a single band coinciding with the lowest molecular weight size. Most likely the secondary band, seen when shgRNA is maintained at RT, represents a dimeric form or an alternative conformational structure. For the purpose of storage, shgRNA was aliquoted and stored at -80^{o}C.

Preparation of Cas9 mRNA – Several versions of engineered Cas9 are currently available. For this study, we opted for a zebrafish-codon optimised Cas9 version derived

from *S. pyogenes*. The Cas9 we used was also engineered to contain (at both its amino and carboxyl termini) a Nuclear Localisation Signal (NLS) derived from the SV40 large T-antigen sequence, which would facilitate translocation of the protein to the cell nucleus. The plasmid used was previously described in reference[15]. In this plasmid, the Cas9 coding sequence is cloned downstream of the SP6 promoter and upstream of an SV40 polyadenylation site and a NotI unique restriction site, which is used for plasmid linearisation prior to *in vitro* transcription. The plasmid was purified using an EndoFree Plasmid Purification (Maxi prep) kit (Qiagen) from 100 ml of O/N culture, and according to manufacturer's guidelines. Total plasmid DNA was suspended in 700 µl and quantified as approximately 1 µg/µl concentration. 25 µg of DNA were linearised with 0.2 units/µl of NotI (New England BioLabs) in 1x NEB Buffer 3.1 for 2 h at 37^{0}C in a 200 µl reaction. Complete digestion was assessed by 1% agarose gel electrophoresis. The linearised plasmid was purified by precipitation by Sodium Acetate/EtOH method. The pellet was washed with 70% EtOH, air-dried and resuspended in 50 µl RNase-free water. The Cas9 mRNA was then synthesised using the mMESSAGE mMACHINE SP6 kit (Invitrogen), according to the manufacturer's guidelines and using 1 µg of purified linearised plasmid as a template for a 20 µl reaction. The mRNA was then column-purified using the RNeasy MiniElute Cleanup kit (Qiagen), eluted in 20 µl (2x10 µl) of RNase-free water and quantified by Nanodrop as approximately 1 µg/µl. The integrity of RNA was assessed by 2% non-denaturing agarose gel electrophoresis, on which Cas9 mRNA appeared with two discrete bands. Single use 2 µl aliquots of 1 µg/µl Cas9 mRNA were stored at -80 ^{0}C.

Zebrafish lines and maintenance – Zebrafish lines were handled in compliance with the local animal welfare regulations and maintained according to standard protocols (zfin.org). The breeding of adult fish was approved by the local animal welfare committee (DEC) of the University of Leiden (license number: 10612) and adhered to the international guidelines specified by the EU Animal Protection Directive 2010/63/EU. Adult zebrafish were not sacrificed for experiments. Fish lines used in this work were the following: wt strain AB/TL and *Tg(fli1a:eGFP^{y1})*[45]. Anaesthesia of embryos/larvae used for live imaging was achieved with 0.02% buffered Tricaine (3-aminobenzoic acid ethyl ester, Sigma-Aldrich) in egg water.

shgRNA/Cas9 microinjections – To assess efficiency and toxicity, eGFP-shgRNA and Cas9 mRNA were mixed and injected at different concentrations, as described in the results section and in **Figure 4**. For generation of the *cxcr3.3* mutant lines, 1 nl of 150 pg of Cas9 mRNA and 150 pg of *cxcr3.3*-shgRNA Target C was considered optimal as this did not lead to toxic/phenotypic effects or major lethality. Injections were performed in the cell of fertilised eggs at 5-10 minutes post fertilisation. Left over mix from the injection needle was run on 2% non-denaturing agarose gel to control integrity during the injection phase. The mix would segregate into 4 bands, 2 corresponding to the Cas9 mRNA and 2 corresponding to the shgRNA.

Genotyping – Genotypes were assessed by PCR using the primers reported in **Supplementary Table 1**, extracting genomic DNA from 1-2 dpf embryos or fin clips of > 6 week-old juveniles/adults. Successful injections were confirmed by Sanger sequencing (Baseclear or Macrogen, The Netherlands). Mutations were identified from heterozygote F1 fish by agarose gel electrophoresis (2-4%) and confirmed by Sanger sequencing from heterozygotes or F2 homozygotes.

Survival analysis – Heterozygotes carrying the same mutation were incrossed to generate homozygote mutants, wt and heterozygotes. The mixed family was cultured to sexual maturity and then genotyped by PCR/gel electrophoresis. No significant divergence from Mendelian proportions was observed in the genotype rates (assessed by chi-squared test).

Infection burden – Homozygote mutants and wt, derived either from heterozygote parents or from homozygote siblings incross, were injected via the blood island at 28-30 hpf with 100-250 CFU of mCherry-labelled *Mycobacterium marinum* M strain. Infection burden was quantified at 4 dpi by fluorescent pixel enumeration as previously described[9]. Significance was assessed by Mann-Whitney test (**Figure 6 C**) and with unpaired t-test with Welch's correction for data with different variances (**Figure 6F,H**). *P<0.05; **P<0.01; ***P<0.001. Error bars: mean±s.e.m.

ACKNOWLEDGEMENTS

We thank Anna-Pavlina Haramis and Rui Zhang for the discussions and the collaboration in setting up the CRISPR/Cas9 technology.

This work was supported by the Smart Mix Program of the Netherlands Ministry of Economic Affairs and the Ministry of Education, Culture and Science, the European Commission 7th framework project ZF-HEALTH (contract number HEALTH-F4-2010-242048), and the European Marie-Curie Initial Training Network FishForPharma (contract number PITN-GA-2011-289209).

Name	Target	Sequence (5'-3')	Method	Short description
eGFP 121-mer	eGFP	GATCCGCACCGACTCGGTGCCACTTTTTCAAGTTGATAACGGACTAGCCTTATTTTAACTTGCTATTTCTAGCTCTAAAACCCGGCAAGCTGCCCGTGCCCCTATAGTGAGTCGTATTACGC	1 and 2	Full length ssDNA oligos used for direct *in vitro* transcription (Method 1) or for generation of PCR templates for shgRNA transcription (Method 2)
cxcr3.3 Target A 122-mer	*cxcr3.3*	GATCCGCACCGACTCGGTGCCACTTTTTCAAGTTGATAACGGACTAGCCTTATTTTAACTTGCTATTTCTAGCTCTAAAACGCAGCCCCAATAAGATCCCCCTATAGTGAGTCGTATTACGC	1 and 2	
cxcr3.3 Target B 122-mer	*cxcr3.3*	GATCCGCACCGACTCGGTGCCACTTTTTCAAGTTGATAACGGACTAGCCTTATTTTAACTTGCTATTTCTAGCTCTAAAACTGCTTTACTCTTTGGGGATCCTATAGTGAGTCGTATTACGC	1 and 2	
T7 promoter primer	all 121-mers	TAATACGACTCACTATAG	1	Primer to complement T7 promoter by annealing to 121-mers
cxcr3.3 Target C 81-mer Fw	*cxcr3.3*	GCGTAATACGACTCACTATAGGACTGGTTCTGGCAGTATTGGTTTTAGAGCTAGAAATAGCAAGTTAAAATAAGGCTAGTC	3	Semi-complementary oligos used for generation of PCR templates for *in vitro* transcription of shgRNA
cxcr3.3 Target D 81-mer Fw	*cxcr3.3*	GCGTAATACGACTCACTATAGGATGTTGGCCTTCATCAGTGGTTTTAGAGCTAGAAATAGCAAGTTAAAATAAGGCTAGTC	3	
Constant 81-mer Rv	all Fw 81-mers	GATCCGCACCGACTCGGTGCCACTTTTTCAAGTTGATAACGGACTAGCCTTATTTTAACTTGCTATTTCTAGCTCTAAAAC	3	
Template amplif. Fw	all PCR templates	GATCCGCACCGACTCGGT	2 and 3	PCR primers to amplify the template for shgRNA transcription
Template amplif. Rv	all PCR templates	GCGTAATACGACTCACTATAG	2 and 3	
eGFP gFw	eGFP	AAACGGCCACAAGTTCAGCG	Genot.	Primers used for PCR genotyping of targeted genomic loci
eGFP gRv	eGFP	TCACCTTGATGCCGTTCTTCTG	Genot.	
cxcr3.3A-B gFw	*cxcr3.3*	ACATGGAGGTAGAGCTTCACGG	Genot.	
cxcr3.3A-B gRv	*cxcr3.3*	CTCACCTTAAACAGAACTCCAGCC	Genot.	
cxcr3.3C gFw	*cxcr3.3*	GAGGTAGAGCTTCACGGATTGT	Genot.	
cxcr3.3C gRv	*cxcr3.3*	GAGAGCAGCAGAAGACTGTCAA	Genot.	
cxcr3.3D gFw	*cxcr3.3*	TAAATTGATTTTAATCGACTTGACG	Genot.	
cxcr3.3D gRv	*cxcr3.3*	AAAGATCCATTCTGGGATGCTA	Genot.	

Supplementary Table 1. Primers and oligos used in this study. Sequences marked in blue correspond to the T7 promoter sequence. Sequences in green represent the target sites. Sequences in orange represent the semi-complementary stretches of the 81-mers used in Method 3.

Supplementary Figure 1. Full sequence alignment of human (hsa) CXCR3 with zebrafish (dre) Cxcr3.1, Cxcr3.2 and Cxcr3.3.

REFERENCES

1 Zlotnik A, Yoshie O. Chemokines: a new classification system and their role in immunity. Immunity. 2000 Feb;12(2):121-7.

2 Torraca V, Masud S, Spaink HP, Meijer AH. Macrophage-pathogen interactions in infectious diseases: new therapeutic insights from the zebrafish host model. Dis Model Mech. 2014 Jul;7(7):785-97.

3 Donà E, Barry JD, Valentin G, Quirin C, Khmelinskii A, Kunze A, Durdu S, Newton LR, Fernandez-Minan A, Huber W, Knop M, Gilmour D. Directional tissue migration through a self-generated chemokine gradient. Nature. 2013 Nov 14;503(7475):285-9.

4 Walters KB, Green JM, Surfus JC, Yoo SK, Huttenlocher A. Live imaging of neutrophil motility in a zebrafish model of WHIM syndrome. Blood. 2010 Oct 14;116(15):2803-11.

5 Busch-Nentwich E, Kettleborough R, Dooley CM, Scahill C, Sealy I, White R, Herd C, Mehroke S, Wali N, Carruthers S, Hall A, Collins J, Gibbons R, Pusztai Z, Clark R, Stemple DL. Sanger Institute Zebrafish Mutation Project mutant data submission. ZFIN Direct Data Submission. 2013.

6 Valentin G, Haas P, Gilmour D. The chemokine SDF1a coordinates tissue migration through the spatially restricted activation of Cxcr7 and Cxcr4b. Curr Biol. 2007 Jun 19;17(12):1026-31.

7 Knaut H, Werz C, Geisler R, Nüsslein-Volhard C; Tübingen 2000 Screen Consortium. A zebrafish homologue of the chemokine receptor Cxcr4 is a germ-cell guidance receptor. Nature. 2003 Jan 16;421(6920):279-82.

8 Lewellis SW, Nagelberg D, Subedi A, Staton A, LeBlanc M, Giraldez A, Knaut H. Precise SDF1-mediated cell guidance is achieved through ligand clearance and microRNA-mediated decay. J Cell Biol. 2013 Feb 4;200(3):337-55.

9 Torraca V, Cui C, Boland R, Bebelman JP, van der Sar AM, Smit MJ, Siderius M, Spaink HP, Meijer AH. The CXCR3-CXCL11 signaling axis mediates macrophage recruitment and dissemination of mycobacterial infection. Dis Model Mech. 2015 Mar;8(3):253-69.
10 Siekmann AF, Standley C, Fogarty KE, Wolfe SA, Lawson ND. Chemokine signaling guides regional patterning of the first embryonic artery. Genes Dev. 2009 Oct1;23(19):2272-7.
11 Bussmann J, Wolfe SA, Siekmann AF. Arterial-venous network formation during brain vascularization involves hemodynamic regulation of chemokine signaling. Development. 2011 May;138(9):1717-26.
12 Jinek M, Chylinski K, Fonfara I, Hauer M, Doudna JA, Charpentier E. A programmable dual-RNA-guided DNA endonuclease in adaptive bacterial immunity. Science. 2012 Aug 17;337(6096):816-21.
13 Mali P, Esvelt KM, Church GM. Cas9 as a versatile tool for engineering biology. Nat Methods. 2013 Oct;10(10):957-63.
14 Ran FA, Hsu PD, Wright J, Agarwala V, Scott DA, Zhang F. Genome engineering using the CRISPR-Cas9 system. Nat Protoc. 2013 Nov;8(11):2281-308.
15 Jao LE, Wente SR, Chen W. Efficient multiplex biallelic zebrafish genome editing using a CRISPR nuclease system. Proc Natl Acad Sci U S A. 2013 Aug 20;110(34):13904-9.
16 Hwang WY, Fu Y, Reyon D, Maeder ML, Tsai SQ, Sander JD, Peterson RT, Yeh JR,Joung JK. Efficient genome editing in zebrafish using a CRISPR-Cas system. Nat Biotechnol. 2013 Mar;31(3):227-9.
17 Hruscha A, Krawitz P, Rechenberg A, Heinrich V, Hecht J, Haass C, Schmid B. Efficient CRISPR/Cas9 genome editing with low off-target effects in zebrafish. Development. 2013 Dec;140(24):4982-7.
18 Auer TO, Del Bene F. CRISPR/Cas9 and TALEN-mediated knock-in approaches in zebrafish. Methods. 2014 Sep;69(2):142-50.
19 Kleinstiver BP, Pattanayak V, Prew MS, Tsai SQ, Nguyen NT, Zheng Z, Joung JK. High-fidelity CRISPR-Cas9 nucleases with no detectable genome-wide off-target effects. Nature. 2016 Jan 28;529(7587):490-5.
20 Nomiyama H, Osada N, Yoshie O. Systematic classification of vertebrate chemokines based on conserved synteny and evolutionary history. Genes Cells. 2013 Jan;18(1):1-16.
21 Lindley I, Aschauer H, Seifert JM, Lam C, Brunowsky W, Kownatzki E, Thelen M, Peveri P, Dewald B, von Tscharner V, et al. Synthesis and expression in Escherichia coli of the gene encoding monocyte-derived neutrophil-activating factor: biological equivalence between natural and recombinant neutrophil-activating factor. Proc Natl Acad Sci U S A. 1988 Dec;85(23):9199-203.
22 Hoffmann E, Dittrich-Breiholz O, Holtmann H, Kracht M. Multiple control of interleukin-8 gene expression. J Leukoc Biol. 2002 Nov;72(5):847-55.
23 de Oliveira S, Reyes-Aldasoro CC, Candel S, Renshaw SA, Mulero V, Calado A. Cxcl8 (IL-8) mediates neutrophil recruitment and behavior in the zebrafish inflammatory response. J Immunol. 2013 Apr 15;190(8):4349-59.
24 Tanino Y, Coombe DR, Gill SE, Kett WC, Kajikawa O, Proudfoot AE, Wells TN, Parks WC, Wight TN, Martin TR, Frevert CW. Kinetics of chemokine-glycosaminoglycan interactions control neutrophil migration into the airspaces of the lungs. J Immunol. 2010 Mar 1;184(5):2677-85.
25 Mukaida N. Pathophysiological roles of interleukin-8/CXCL8 in pulmonary diseases. Am J Physiol Lung Cell Mol Physiol. 2003 Apr;284(4):L566-77.
26 Nagasawa T, Hirota S, Tachibana K, Takakura N, Nishikawa S, Kitamura Y, Yoshida N, Kikutani H, Kishimoto T. Defects of B-cell lymphopoiesis and bone-marrow myelopoiesis in mice lacking the CXC chemokine PBSF/SDF-1. Nature. 1996 Aug 15;382(6592):635-8.
27 Sallusto F, Baggiolini M. Chemokines and leukocyte traffic. Nat Immunol. 2008 Sep;9(9):949-52.
28 Balkwill F. The significance of cancer cell expression of the chemokine receptor CXCR4. Semin Cancer Biol. 2004 Jun;14(3):171-9.
29 Feng Y, Broder CC, Kennedy PE, Berger EA. HIV-1 entry cofactor: functionalcDNA cloning of a seven-transmembrane, G protein-coupled receptor. Science. 1996 May 10;272(5263):872-7.
30 Tamplin OJ, Durand EM, Carr LA, Childs SJ, Hagedorn EJ, Li P, Yzaguirre AD, Speck NA, Zon LI. Hematopoietic stem cell arrival triggers dynamic remodeling of the perivascular niche. Cell. 2015 Jan 15;160(1-2):241-52.
31 Tulotta C, Stefanescu C, Beletkaia E, Bussmann J, Tarbashevich K, Schmidt T,Snaar-Jagalska BE. Inhibition of signaling between human CXCR4 and zebrafishligands by the small molecule IT1t impairs the formation of triple-negativebreast cancer early metastases in a zebrafish xenograft model. Dis Model Mech.2016 Feb 1;9(2):141-53.
32 Chong SW, Emelyanov A, Gong Z, Korzh V. Expression pattern of two zebrafish genes, cxcr4a and cxcr4b. Mech Dev. 2001 Dec;109(2):347-54.
33 Nagasawa T, Nakajima T, Tachibana K, Iizasa H, Bleul CC, Yoshie O, Matsushima K, Yoshida N, Springer TA, Kishimoto T. Molecular cloning and characterization of a murine pre-B-cell growth-stimulating

factor/stromal cell-derived factor 1 receptor, a murine homolog of the human immunodeficiency virus 1 entry coreceptor fusin. Proc Natl Acad Sci U S A. 1996 Dec 10;93(25):14726-9.
34 Tachibana K, Hirota S, Iizasa H, Yoshida H, Kawabata K, Kataoka Y, Kitamura Y,Matsushima K, Yoshida N, Nishikawa S, Kishimoto T, Nagasawa T. The chemokine receptor CXCR4 is essential for vascularization of the gastrointestinal tract. Nature. 1998 Jun 11;393(6685):591-4.
35 Zou YR, Kottmann AH, Kuroda M, Taniuchi I, Littman DR. Function of the chemokine receptor CXCR4 in haematopoiesis and in cerebellar development. Nature. 1998 Jun 11;393(6685):595-9.
36 Zhou J, Tang PC, Qin L, Gayed PM, Li W, Skokos EA, Kyriakides TR, Pober JS,Tellides G. CXCR3-dependent accumulation and activation of perivascular macrophages is necessary for homeostatic arterial remodeling to hemodynamic stresses. J Exp Med. 2010 Aug 30;207(9):1951-66.
37 Krauthausen M, Kummer MP, Zimmermann J, Reyes-Irisarri E, Terwel D, Bulic B, Heneka MT, Müller M. CXCR3 promotes plaque formation and behavioral deficits in an Alzheimer's disease model. J Clin Invest. 2015 Jan;125(1):365-78.
38 Oghumu S, Varikuti S, Terrazas C, Kotov D, Nasser MW, Powell CA, Ganju RK,Satoskar AR. CXCR3 deficiency enhances tumor progression by promoting macrophage M2 polarization in a murine breast cancer model. Immunology. 2014 Sep;143(1):109-19.
39 Cohen SB, Maurer KJ, Egan CE, Oghumu S, Satoskar AR, Denkers EY. CXCR3-dependent $CD4^+$ T cells are required to activate inflammatory monocytes for defense against intestinal infection. PLoS Pathog. 2013;9(10):e1003706.
40 Torraca V, in't Veld E, Meijer AH. Disruption of chemotactic signalling primes the lysosomal function of macrophages to counteract mycobacterial parasitism. *Chapter 4 of this thesis*.
41 Cui C. Chemokine signaling in innate immunity of zebrafish embryos. Doctoral Thesis, Leiden University. 2012 Dec 20.
42 Montague TG, Cruz JM, Gagnon JA, Church GM, Valen E. CHOPCHOP: a CRISPR/Cas9 and TALEN web tool for genome editing. Nucleic Acids Res. 2014 Jul;42(Web Server issue):W401-7.
43 Langmead B, Trapnell C, Pop M, Salzberg SL. Ultrafast and memory-efficient alignment of short DNA sequences to the human genome. Genome Biol. 2009;10(3):R25.
44 Wang T, Wei JJ, Sabatini DM, Lander ES. Genetic screens in human cells using the CRISPR-Cas9 system. Science. 2014 Jan 3;343(6166):80-4.
45 Lawson ND, Weinstein BM. In vivo imaging of embryonic vascular developmentusing transgenic zebrafish. Dev Biol. 2002 Aug 15;248(2):307-18.
46 Grone BP, Marchese M, Hamling KR, Kumar MG, Krasniak CS, Sicca F, Santorelli FM, Patel M, Baraban SC. Epilepsy, Behavioral Abnormalities, and Physiological Comorbidities in Syntaxin-Binding Protein 1 (STXBP1) Mutant Zebrafish. PLoS One. 2016 Mar 10;11(3):e0151148.
47 D'Agostino Y, Locascio A, Ristoratore F, Sordino P, Spagnuolo A, Borra M, D'Aniello S. A Rapid and Cheap Methodology for CRISPR/Cas9 Zebrafish Mutant Screening. Mol Biotechnol. 2016 Jan;58(1):73-8.
48 Taylor SM, Alvarez-Delfin K, Saade CJ, Thomas JL, Thummel R, Fadool JM, Hitchcock PF. The bHLH Transcription Factor NeuroD Governs Photoreceptor Genesis and Regeneration Through Delta-Notch Signaling. Invest Ophthalmol Vis Sci. 2015 Nov;56(12):7496-515.
49 Chang N, Sun C, Gao L, Zhu D, Xu X, Zhu X, Xiong JW, Xi JJ. Genome editing with RNA-guided Cas9 nuclease in zebrafish embryos. Cell Res. 2013 Apr;23(4):465-72.
50 Yu C, Zhang Y, Yao S, Wei Y. A PCR based protocol for detecting indel mutations induced by TALENs and CRISPR/Cas9 in zebrafish. PLoS One. 2014 Jun 5;9(6):e98282.
51 Irion U, Krauss J, Nüsslein-Volhard C. Precise and efficient genome editing in zebrafish using the CRISPR/Cas9 system. Development. 2014 Dec;141(24):4827-30.
52 Varshney GK, Pei W, LaFave MC, Idol J, Xu L, Gallardo V, Carrington B, Bishop K, Jones M, Li M, Harper U, Huang SC, Prakash A, Chen W, Sood R, Ledin J, Burgess SM. High-throughput gene targeting and phenotyping in zebrafish using CRISPR/Cas9. Genome Res. 2015 Jul;25(7):1030-42.
53 Brocal I, White RJ, Dooley CM, Carruthers SN, Clark R, Hall A, Busch-Nentwich EM, Stemple DL, Kettleborough RN. Efficient identification of CRISPR/Cas9-induced insertions/deletions by direct germline screening in zebrafish. BMC Genomics. 2016 Mar 24;17(1):259.
54 Arnaud-Barbe N, Cheynet-Sauvion V, Oriol G, Mandrand B, Mallet F. Transcription of RNA templates by T7 RNA polymerase. Nucleic Acids Res. 1998 Aug 1;26(15):3550-4.
55 Ran FA, Hsu PD, Wright J, Agarwala V, Scott DA, Zhang F. Genome engineering using the CRISPR-Cas9 system. Nat Protoc. 2013 Nov;8(11):2281-308.
56 Nomiyama H, Yoshie O. Functional roles of evolutionary conserved motifs and residues in vertebrate chemokine receptors. J Leukoc Biol. 2015 Jan;97(1):39-47

57 Lagane B, Ballet S, Planchenault T, Balabanian K, Le Poul E, Blanpain C, Percherancier Y, Staropoli I, Vassart G, Oppermann M, Parmentier M, Bachelerie F. Mutation of the DRY motif reveals different structural requirements for the CC chemokine receptor 5-mediated signaling and receptor endocytosis. Mol Pharmacol. 2005 Jun;67(6):1966-76.
58 Rovati GE, Capra V, Neubig RR. The highly conserved DRY motif of class A G protein-coupled receptors: beyond the ground state. Mol Pharmacol. 2007 Apr;71(4):959-64.
59 Acharya S, Karnik SS. Modulation of GDP release from transducin by the conserved Glu134-Arg135 sequence in rhodopsin. J Biol Chem. 1996 Oct 11;271(41):25406-11.
60 Cancellieri C, Vacchini A, Locati M, Bonecchi R, Borroni EM. Atypical chemokine receptors: from silence to sound. Biochem Soc Trans. 2013 Feb 1;41(1):231-6.
61 Nygaard R, Frimurer TM, Holst B, Rosenkilde MM, Schwartz TW. Ligand binding and micro-switches in 7TM receptor structures. Trends Pharmacol Sci. 2009 May;30(5):249-59.
62 Auger GA, Pease JE, Shen X, Xanthou G, Barker MD. Alanine scanning mutagenesis of CCR3 reveals that the three intracellular loops are essential for functional receptor expression. Eur J Immunol. 2002 Apr;32(4):1052-8.
63 Zou J, Redmond AK, Qi Z, Dooley H, Secombes CJ. The CXC chemokine receptors of fish: Insights into CXCR evolution in the vertebrates. Gen Comp Endocrinol. 2015 May 1;215:117-31.
64 Ulvmar MH, Hub E, Rot A. Atypical chemokine receptors. Exp Cell Res. 2011 Mar 10;317(5):556-68.
65 Nibbs R, Graham G, Rot A. Chemokines on the move: control by the chemokine "interceptors" Duffy blood group antigen and D6. Semin Immunol. 2003 Oct;15(5):287-94.
66 Mantovani A, Bonecchi R, Locati M. Tuning inflammation and immunity by chemokine sequestration: decoys and more. Nat Rev Immunol. 2006 Dec;6(12):907-18.
67 Fra AM, Locati M, Otero K, Sironi M, Signorelli P, Massardi ML, Gobbi M, Vecchi A, Sozzani S, Mantovani A. Cutting edge: scavenging of inflammatory CC chemokines by the promiscuous putatively silent chemokine receptor D6. J Immunol. 2003 Mar 1;170(5):2279-82.
68 Dambly-Chaudière C, Cubedo N, Ghysen A. Control of cell migration in the development of the posterior lateral line: antagonistic interactions between the chemokine receptors CXCR4 and CXCR7/RDC1. BMC Dev Biol. 2007 Mar 29;7:23.
69 Naumann U, Cameroni E, Pruenster M, Mahabaleshwar H, Raz E, Zerwes HG, Rot A, Thelen M. CXCR7 functions as a scavenger for CXCL12 and CXCL11. PLoS One. 2010 Feb 11;5(2):e9175.
70 Bamberg CE, Mackay CR, Lee H, Zahra D, Jackson J, Lim YS, Whitfeld PL, Craig S, Corsini E, Lu B, Gerard C, Gerard NP. The C5a receptor (C5aR) C5L2 is a modulator of C5aR-mediated signal transduction. J Biol Chem. 2010 Mar 5;285(10):7633-44.
71 Di Liberto D, Locati M, Caccamo N, Vecchi A, Meraviglia S, Salerno A, Sireci G, Nebuloni M, Caceres N, Cardona PJ, Dieli F, Mantovani A. Role of the chemokine decoy receptor D6 in balancing inflammation, immune activation, and antimicrobial resistance in Mycobacterium tuberculosis infection. J Exp Med. 2008 Sep 1;205(9):2075-84.